



Australian Government
Department of Defence
Defence Science and
Technology Organisation

Phased Array Radar Data Processing Using Adaptive Displaced Phase Centre Antenna Principle

Yunhan Dong

Electronic Warfare and Radar Division
Defence Science and Technology Organisation

DSTO-RR-0334

ABSTRACT

Employing the autoregressive (AR) technique and the principle of displaced phase centre antenna (DPCA) we construct an optimum adaptive DPCA processor for moving target detection from airborne phased array radar data collected under non-DPCA conditions. It is fundamentally different from the existing adaptive DPCA which is not optimum. The number of range samples it needs to estimate its parameters is only approximately twice the number of antenna elements, significantly smaller than the number required by the conventional space-time adaptive processing (STAP) and other algorithms. Computationally it only requires 5-10% cost of STAP. The processor is tested using both the simulated and genuine airborne phased array radar data. With ample samples, its performance approaches optimum. In the case of reduced samples, it considerably outperforms STAP and others examined.

APPROVED FOR PUBLIC RELEASE

Published by

*Defence Science and Technology Organisation
PO Box 1500
Edinburgh South Australia 5111*

*Telephone: (08) 8259 5555
Fax: (08) 8259 6567*

*© Commonwealth of Australia 2007
AR-014-074
December 2007*

APPROVED FOR PUBLIC RELEASE

Phased Array Radar Data Processing Using Adaptive Displaced Phase Centre Antenna Principle

EXECUTIVE SUMMARY

The Australian Defence Force (ADF) is acquiring an Airborne Early Warning and Control (AEW&C) capability under Project AIR 5077 (Project Wedgetail). The AEW&C aircraft is equipped with an L-band phased array radar system for moving target detection. An electronically scanned phased array antenna offers rugged, reliable and comprehensive detection potential. However, how to process massive phased array radar data in given time frames remains a key issue in phased array radar data processing.

Although space-time adaptive processing (STAP) has attracted a lot of attention in the research literature, its computational demands have limited its application in real-time airborne radar systems. In this report we investigate a new technique for adaptive displaced phase centre antenna (ADPCA) clutter cancellation which yields almost as good a performance as STAP at a fraction of the computational cost. In regions of limited data samples it is superior to STAP.

STAP yields the optimum signal-to-interference-and-noise ratio (SINR) for detection of moving targets embedded in Gaussian distributed thermal noise, clutter (echoes from the Earth's surface) and broadband noise jamming. However, there are two critical issues in real-time implementation of STAP in airborne radar systems. First it needs a large number of range samples to estimate the covariance matrix of the undesired signals, which may not be met sometimes. The second and the more critical issue is the computational requirement. The dominant computation in STAP is the inversion of the covariance matrix which is not only computationally expensive, but also a nonlinear transform making parallel processing difficult if not impossible. Numerous algorithms, aimed at reducing computational cost and sample data requirement have been proposed in the past.

Displaced phase centre antenna (DPCA) processing is a technique for countering the platform motion induced clutter spectrum spreading. The basic concept is to make the antenna appear stationary even though the platform is moving forward by

electronically shifting the receive aperture backwards during the operation. Since its origins in the 1950s at General Electric where it was applied to airborne early warning (AEW) radars, various DPCA techniques have been developed. For airborne radars a typical way to achieve this is to adjust the radar pulse repetition frequency (PRF) according to the platform velocity so that the first, second, etc. antenna elements at the current pulse effectively move to, respectively, the exact positions of the second, third, etc. antenna elements at the previous pulse, and so on. This is often referred to as the DPCA condition. In practice, even if the DPCA condition is satisfied, the clutter cancellation is still limited, due to various disturbances introduced by the radar (such as imbalance among antenna channels and phase errors, etc.), platform (instability of velocity and crabbing, etc.), and clutter environment (clutter intrinsic motion). To overcome these issues, the so-called ADPCA concept has been introduced. However to construct an ADPCA processor for airborne phased array radars is not as easy as it seems. The existing version of ADPCA was developed about ten years ago. Unfortunately, we prove that this existing ADPCA is not an optimum processor and could lead to significant SINR loss.

Inspired by the DPCA and parametric adaptive matched filtering (PAMF) approaches, this report derives another ADPCA algorithm which is fundamentally different from its predecessor. Unlike the existing one which is not optimum, the proposed ADPCA has its roots in the autoregressive (AR) process and is an optimum processor. It is mathematically similar to the PAMF approach, but has some advantages over the PAMF processor. The approach does not require the DPCA condition because its parameters are adaptively estimated, which automatically takes account of non-DPCA conditions as well as various other disturbances. It significantly reduces the size of sample data needed to estimate its parameters and the computational cost compared to its predecessors and STAP.

The performance of the algorithm has been assessed using two airborne radar datasets, one generated using the high fidelity airborne radar simulation software, RLSTAP, and the other collected by the Multi-Channel Airborne Radar Measurements (MCARM) system. These two datasets were carefully chosen to cover various issues. First of all, the datasets did not satisfy the DPCA condition, so that the adaptability of the proposed ADPCA could be examined. Secondly the radar did not look in the broadside direction in the RLSTAP dataset. The second dataset was collected from a flight trial of MCARM and included the effects of aircraft crabbing motion (the crab angle is as large as 7 degrees). Other decorrelation effects, including radar instability, clutter intrinsic motion, range foldover and interference caused by the aircraft etc., were automatically included in the dataset. Therefore the evaluation of the proposed processor is realistic. The results of STAP have served as benchmarks in evaluation.

It has been found that the proposed ADPCA performs nearly as well as STAP, suffering at most a few dB of processing gain loss in the vicinity of the Doppler of the mainlobe clutter. However if there are insufficient clutter samples to accurately

estimate the covariance matrix, the performance of STAP is severely degraded whereas the proposed ADPCA still performs as well as before. Mathematically STAP requires an estimation of its covariance matrix whose size is the product of the number of antenna elements and the number of pulses in a CPI. On the other hand, the proposed ADPCA estimates its parameters by the use of covariance matrices whose size is no more than the number of antenna elements. In addition, in estimating parameters, STAP uses averaging processing only in the fast-time domain, whereas the proposed ADPCA utilises averaging processing in both the fast-time and the low-time domains. These two differences make the proposed ADPCA more robust and require much less sample data. In general, the parameters of ADPCA can be satisfactorily estimated once the number of range samples is equal to or greater than twice of the antenna elements. The existing ADPCA, on the other hand, is not an optimum processor and its performance usually is poor and suffers significantly especially when the target's Doppler is close to that of the mainlobe clutter.

The computational cost of the proposed ADPCA has been estimated. In general, it only has approximately 5-10% of the computational cost of STAP. Since most of the computation in the ADPCA algorithm is linear transforms, parallel processing and/or hardware realisation can be easily implemented. In contrast, the dominant calculation of the STAP algorithm is the inversion of the covariance matrix which is not a linear transform and limits the application of parallel processing. In this sense, the computational savings of the ADPCA algorithm is even greater than the simple estimation of operational counts presented in the report.

In conclusion, the proposed ADPCA algorithm has significant advantages in requiring far fewer samples and much less computation while achieving robust performance with the SINR improvement close to optimal. It therefore has a great potential to be implemented in real-time airborne radar systems.

Author

Yunhan Dong

Electronic Warfare Division

Dr Yunhan Dong received his Bachelor and Master degrees in 1980s in China and his PhD in 1995 at UNSW, Australia, all in electrical engineering. He then worked at UNSW from 1995 to 2000, and Optus Telecommunications Inc from 2000 to 2002. He joined DSTO as a Senior Research Scientist in 2002. His research interests are primarily in radar signal and image processing, and radar backscatter modelling. Dr Dong was a recipient of both Postdoctoral Research Fellowships and Research Fellowships from the Australian Research Council.

Contents

| | | |
|-------|---|----|
| 1. | INTRODUCTION | 1 |
| 2. | SPACE-TIME ADAPTIVE PROCESSING | 3 |
| 3. | CLASSICAL DISPLACED PHASE CENTRE ANTENNA | 6 |
| 3.1 | Displaced Phase Centre Antenna | 6 |
| 3.2 | Blum's Adaptive DPCA | 8 |
| 4. | PROPOSED ADAPTIVE DISPLACED PHASE CENTRE ANTENNA | 12 |
| 4.1 | Formulation of Proposed ADPCA | 12 |
| 4.2 | Two Significant Advantages of Proposed ADPCA over STAP | 16 |
| 4.2.1 | Computational Savings | 16 |
| 4.2.2 | Robustness of Proposed ADPCA | 19 |
| 4.2.3 | Inherent SINR Loss of ADPCA | 20 |
| 5. | PERFORMANCE ASSESSMENT | 20 |
| 5.1 | RLSTAP Dataset | 20 |
| 5.1.1 | Comparison with PAMF | 30 |
| 5.2 | MCARM Dataset | 32 |
| 6. | CONCLUSIONS | 38 |
| 7. | ACKNOWLEDGEMENT | 39 |
| 8. | REFERENCES | 39 |
| | Table 1: Ops required for the STAP process. | 17 |
| | Table 2: Ops required for the proposed ADPCA process. | 18 |
| | Table 3: Parameters used in RLSTAP for generating the simulated airborne radar dataset. | 21 |
| | Table 4: Parameters of targets. | 21 |

| | |
|---|----|
| Table 5: MCARM radar parameters. | 32 |
| Table 6: MCARM platform parameters. | 32 |
| Figure 1: Geometry of a linear airborne antenna array. | 7 |
| Figure 2: Effective array positions for successive pulses of a CPI with $\beta = 1$. | 8 |
| Figure 3: Ratio in percentage of the proposed ADPCA ops to the STAP ops with the parameters of $K = 100$ and $K_{rg} = 500$. | 19 |
| Figure 4: The LULC data superposed on the DTE data of the Washington D. C. area. | 22 |
| Figure 5: Performance comparison between (a) STAP, (b) DPCA, (c) Blum's ADPCA and (d) proposed ADPCA for the RLSTAP data using 267 range samples in forming the covariance matrix. | 23 |
| Figure 6: Performance comparison between (a) STAP, (b) DPCA, (c) Blum's ADPCA and (d) proposed ADPCA for the RLSTAP data using 267 range samples in forming the covariance matrix. The results are plotted in the signal level versus range with the Doppler bins collapsed onto the range. | 24 |
| Figure 7: Performance comparison between (a) STAP, (b) Blum's ADPCA and (c) proposed ADPCA for the RLSTAP data using 100 range samples in forming the covariance matrix. | 25 |
| Figure 8: Performance comparison between (a) STAP, (b) Blum's ADPCA and (c) proposed ADPCA for the RLSTAP data using 100 range samples in forming the covariance matrix. The results are plotted in signal level versus range with the Doppler bins collapsed onto the range. | 26 |
| Figure 9: Performance comparison between (a) STAP, (b) Blum's ADPCA and (c) proposed ADPCA for the RLSTAP data using 50 range samples in forming the covariance matrix. | 27 |
| Figure 10: Performance comparison between (a) STAP, (b) Blum's ADPCA and (c) proposed ADPCA for the RLSTAP data using 50 range samples in forming the covariance matrix. The results are plotted in the signal level versus range with the Doppler bins collapsed onto the range. | 28 |
| Figure 11: Results of the proposed ADPCA without using slow-time averaging processing. | 29 |
| Figure 12: Eigenvalues, in descending order, of the sampled clutter covariance matrix using 800 range samples. | 30 |
| Figure 13: Performance of the PAMF processor with different filtering orders. | 31 |

- Figure 14: Performance of the PAMF processor is dependent on the filtering order. The results are plotted in the signal level versus range with the Doppler bins collapsed onto the range. 32
- Figure 15: Clutter profile in range after the $1/R^3$ range effect was compensated. 33
- Figure 16: Detection results of MCARM data by the use of (a) STAP, (b) Blum's ADPCA and (c) proposed ADPCA. The covariance matrix was formed using approximately 400 range samples. 34
- Figure 17: Detection results of MCARM data by the use of (a) STAP, (b) Blum's ADPCA and (c) proposed ADPCA. The covariance matrix was formed using approximately 400 range samples. The results are plotted in the signal level versus range with the Doppler bins collapsed into the range. 35
- Figure 18: Detection results of MCARM data by the use of (a) STAP, (b) Blum's ADPCA and (c) proposed ADPCA. The covariance matrix was formed using 21 range samples. 36
- Figure 19: Detection results of MCARM data by the use of (a) STAP, (b) Blum's ADPCA and (c) proposed ADPCA. The covariance matrix was formed using 21 range samples. The results are plotted in the signal level versus range with the Doppler bins collapsed into the range. 37

1. Introduction

The Australian Defence Force (ADF) is acquiring an Airborne Early Warning and Control (AEW&C) capability under Project AIR 5077 (Project Wedgetail). The AEW&C aircraft is equipped with an L-band phased array radar system for moving target detection. An electronically scanned phased array antenna offers rugged, reliable and comprehensive detection potential. However, how to process massive phased array radar data in given time frames remains a key issue in phased array radar data processing.

Although space-time adaptive processing (STAP) has attracted a lot of attention in the research literature, its computational demands have limited its application in real-time airborne radar systems. In this report we investigate a new technique for adaptive displaced phase centre antenna (ADPCA) clutter cancellation which yields almost as good a performance as STAP at a fraction of the computational cost. In regions of limited data samples it is superior to STAP.

This Section briefly reviews techniques and problems in this area in connection with the technique to be introduced.

STAP yields the optimum signal-to-interference-and-noise ratio (SINR) for detection of moving targets embedded in Gaussian distributed thermal noise, clutter (echoes from the Earth's surface) and broadband noise jamming (Ward, 1994, Klemm, 2002). However, there are two critical issues in the real-time implementation of STAP in airborne radar systems. First for a range cell (or range cells) under test (CUT), data from a large number of adjacent range cells are required in order to compute the covariance matrix of the undesired signals. The available sample cells are sometimes fewer than required for accurate estimation of the covariance matrix. This, however, may be partially solved by assuming the structure of the covariance matrix to be known (Steiner and Gerlach, 1998, 2000, Gerlach and Picciolo, 2003, Bresler, 1988). The second and more critical issue is the computational requirement. The dominant computation in STAP is the inversion of the covariance matrix, which is a nonlinear transform making parallel processing difficult if not impossible. Numerous algorithms, aimed at reducing the requirement of either sample data or computational cost or both have been proposed (Klemm, 2004, Guerri, 2003, Wang and Cai, 1994, Ward and Kogon, 2004, Wang et al, 2003). Most of these algorithms, however, are based on various assumptions, hence they are confined in a sub-space and only partially-adaptive (Ward, 1994).

Applying space-time non-adaptive processing techniques is another alternative to minimise real-time computational demand. Noticing the natural characteristics of the clutter ridge lying across the Doppler-azimuth plane, Farina et al (1998) have

constructed a nonlinear, non-adaptive space-time processor which incorporates a set of filters with different notch widths corresponding to different space-time correlation coefficients. In application, input data are passed through the set of filters and the filter with the minimum estimated clutter output power is selected as the best filter for the particular input data. Using the displaced phase centre antenna (DPCA) principle, Richardson (1994) has shown that the inverse of the covariance matrix (ICM) has an asymptotic solution, and consequently constructed an optimum weighting vector for an airborne radar system satisfying the DPCA condition. Dong (2005) has proven that the ICM is approximately independent of the clutter environment. As a result, a pre-built space-time non-adaptive processor has been proposed.

Employing the autoregressive (AR) technique (Marple, Jr, 1987), Roman et al (2000) have adapted the parametric filtering concept to processing phased array radar data, and consequently proposed an approach, called parametric adaptive matched filtering (PAMF) (Roman et al, 2000, Michels et al, 2003, Rangaswamy and Michels, 1997, Rangaswamy et al, 1995, Robey et al, 1992, Roman et al, 1997). The key concept in this approach is that measurements of pulse m are estimated using previous measurements of pulses $m-1, m-2, \dots, m-p$ (p is also referred to as the order of the filter, $p \geq 1$). The residue, i.e., the difference between the actual measurement of pulse m and the estimated measurement from previous measurements of pulses $m-1, m-2, \dots, m-p$, is then processed. Since the residue is uncorrelated, its covariance matrix becomes a block diagonal matrix, which in turn significantly simplifies the processing and reduces the requirement of computation. This technique has been reviewed in detail and further developed by Dong (2006).

DPCA processing is a technique for countering the platform motion induced clutter spectrum spreading. The basic concept is to make the antenna appear stationary even though the platform is moving forward by electronically shifting the receive aperture backwards during the operation (Morris and Harkness, 1996). Since DPCA had its origins in the 1950s at General Electric and was applied to airborne early warning (AEW) radars, various DPCA techniques have been developed (Muehe and Labitt, 2000, Nohara, 1995). A typical way to achieve this is to adjust the radar pulse repetition frequency (PRF) according to the platform velocity so that the first, second etc. antenna elements at pulse m effectively move to the respective positions of the second, third etc. antenna elements at pulse $m-1$, and so on. This is often referred to as the DPCA condition. In practice, even if the DPCA condition is satisfied, the clutter cancellation is still limited, due to various disturbances introduced by the radar (such as imbalance among antenna channels and phase errors, etc.), platform (instability of velocity and crabbing, etc.), and clutter environment (clutter intrinsic motion). To overcome these issues, the so-called ADPCA algorithm has been introduced in airborne side-looking linear array radars (Blum et al, 1996, Klemm 2002, Chapter 7, Guerici, 2003, Chapter 5). Unfortunately, we show that it is not an optimum processor in Section 3 and

consequently could have significant SINR loss in Section 5. We refer to this ADPCA as Blum's ADPCA in this report.

Inspired by the DPCA and PAMF approaches, this report proposes another version of ADPCA algorithm applicable to airborne side-looking phased array radar data processing for moving target detection. Although the name of ADPCA has frequently appeared in the literature, the technique developed here is fundamentally different from the existing ones. Unlike the Blum ADPCA which is not optimum, the ADPCA to be introduced here has its roots in the autoregressive (AR) process (Marple, Jr, 1987), and is mathematically similar to the PAMF approaches, but has some advantages over the PAMF processor (refer to Section 5 for the comparison). The approach does not require the DPCA condition, because its parameters are adaptively estimated, which automatically takes account of non-DPCA conditions as well as various other disturbances induced. It significantly reduces the size of sample data needed to estimate its parameters and the computational cost compared to its predecessors. There are no assumptions about the form of the clutter in the algorithm, so it is fully-adaptive. Most importantly the SINR of the processor approaches the optimum.

Section 2 briefly reviews STAP. When sufficient samples are available to accurately estimate the covariance matrix, STAP yields the optimum SINR, and thus serves as a benchmark for evaluating the results of the proposed algorithm. Following the introduction of DPCA and Blum's ADPCA in Section 3, Section 4 formulates the proposed ADPCA algorithm. Its advantages including the requirement of much fewer samples in estimating its parameters as well as the computational savings are also explained and analysed in Section 4. Evaluation of the algorithm is presented in Section 5. Two datasets, one generated using the high fidelity airborne radar simulation software, RLSTAP, and the other collected by the Multi-Channel Airborne Radar Measurements (MCARM) system are used in the assessment, with the results of STAP as benchmarks. The results of the Blum ADPCA and traditional DPCA with non-adaptability are also shown for comparison. Finally Section 6 concludes the report.

2. Space-Time Adaptive Processing

This section briefly reviews the STAP principle as this helps understanding the proposed ADPCA later.

The mathematical notation used in this report follows the convention: boldface uppercase and lowercase letters represent matrices and vectors, respectively, superscripts T , H and $*$ denote transpose, Hermitian transpose and complex conjugate, respectively, and \mathbb{C} and \mathbb{R} stand for the complex and real number fields, respectively. For instance, $\mathbf{x} \in \mathbb{C}^{MN \times 1}$ denotes \mathbf{x} to be an MN -element complex-valued column vector, and $\mathbf{A} \in \mathbb{C}^{MN \times MN}$ denotes \mathbf{A} to be an $MN \times MN$ -element complex-valued matrix. The symbol \otimes denotes the Kronecker matrix product, and $E\{\cdot\}$

expectation. The ensemble average symbol is an over-hat $\hat{\cdot}$, an indication of an estimate of $E\{\cdot\}$ in calculation using finite samples. Uppercases M and N are reserved for the number of pulses in a coherent processing interval (CPI) and the number of antenna elements in azimuth.

In signal processing, one often has to estimate unknown parameters. For instance, the true covariance matrix \mathbf{R}_u which is in practice unknown, is often estimated from range samples by using the maximum likelihood method. The estimated covariance matrix is $\hat{\mathbf{R}}_u$. In consequence the weighting vector of a processor is \mathbf{w} corresponding to \mathbf{R}_u , $\hat{\mathbf{w}}$ corresponding to $\hat{\mathbf{R}}_u$, and so on. Mathematically if the true covariance matrix \mathbf{R}_u is known, the optimum weighting vector of STAP is $\mathbf{w}_{STAP} = \gamma \mathbf{R}_u^{-1} \mathbf{e}$ whereas the estimate is $\hat{\mathbf{w}}_{STAP} = \gamma \hat{\mathbf{R}}_u^{-1} \mathbf{e}$. In order to reduce the number of equations and expressions, this report does not generally discriminate between $\hat{\mathbf{w}}$ and \mathbf{w} , if meanings in the context are clear and often the over-hat (indicating an estimate rather than the true value) will be omitted. In general, when we deal with mathematical derivations, we assume the true values of parameters are known so symbols are without the over-hat. On the other hand, when we come to calculation or realisation, any parameters estimated from using finite sample data should have the over-hat to indicate the approximation or realisation. However if there is no confusion, we will not repeat expressions with the over-hat.

Let the snapshot $\mathbf{x} = [\mathbf{x}^T(0) \quad \mathbf{x}^T(1) \quad \cdots \quad \mathbf{x}^T(M-1)]^T$ with $\mathbf{x}(m) \in \mathbb{C}^{N \times 1}$ be the complex valued sequence of the output of a linear equispaced N -element array after demodulation and pulse compression, corresponding to the return from a single range cell over an M -pulse CPI. If undesired signals \mathbf{x}_u are Gaussian distributed, it is well known that the optimal (i.e., STAP) weighting vector is (Compton, Jr, 1988, Ward, 1994),

$$\mathbf{w}_{opt} = \gamma \mathbf{R}_u^{-1} \mathbf{e} \quad (1)$$

where γ is an arbitrary scalar, which, without loss of generality, we will let equal 1 and hence omit in the following equations. $\mathbf{R}_u = E\{\mathbf{x}_u \mathbf{x}_u^H\} \in \mathbb{C}^{MN \times MN}$ is the covariance matrix of the undesired signals. The undesired signals \mathbf{x}_u may consist of Gaussian distributed clutter, thermal noise and possibly point-source wideband noise jamming. The covariance matrix is generally unknown and often has to be estimated by the use of range samples via the so-called diagonally loaded sample matrix inversion (DL-SMI) method (Carlson, 1988, Ward and Kogon, 2004), as,

$$\hat{\mathbf{R}}_u = \frac{1}{K} \sum_{k=1}^K \mathbf{x}_k \mathbf{x}_k^H + \delta \mathbf{I} \quad (2)$$

where the subscript k denotes range bins, δ is a small value of the order of the system thermal noise level and \mathbf{I} is the identity matrix. The vector $\mathbf{e} \in \mathbb{C}^{MN \times 1}$ is the desired signal spatial-temporal steering vector.

$$\mathbf{e} = \mathbf{e}(f_{td}) \otimes \mathbf{e}(f_{ts}) \quad (3)$$

where f_{td} and f_{ts} are the normalised target Doppler and spatial (azimuth) frequencies, respectively. Vectors $\mathbf{e}(f_{td})$ and $\mathbf{e}(f_{ts})$ are the desired target temporal and spatial steering vectors, respectively, defined as,

$$\mathbf{e}(f_{td}) = \frac{1}{\sqrt{M}} [1 \quad \exp(j2\pi f_{td}) \quad \cdots \quad \exp(j2\pi(M-1)f_{td})]^T \quad (4)$$

and

$$\mathbf{e}(f_{ts}) = \frac{1}{\sqrt{N}} [1 \quad \exp(j2\pi f_{ts}) \quad \cdots \quad \exp(j2\pi(N-1)f_{ts})]^T \quad (5)$$

Using block component notation, (3) may be written as,

$$\mathbf{e}(m) = \frac{1}{\sqrt{M}} \exp(j2\pi m f_{td}) \mathbf{e}(f_{ts}) \quad m = 0, 1, \dots, M-1 \quad (6)$$

The output of the optimum processor is the product of the Hermitian transpose of the optimal weighting vector times the data snapshot,

$$y = \mathbf{w}_{opt}^H \mathbf{x} \quad (7)$$

The coherent processing gain of the STAP processor approaches the upper limit, $10\log_{10}(MN)$ dB, for deterministic signals whose bearings differ from the jamming bearings, and whose Doppler frequencies differ from the Doppler frequency of clutter in the radar look direction.

Given a target signal $\alpha \mathbf{e}$, where α is the amplitude of the target signal, the SINR is defined as the ratio of the output target power to the output interference and noise power,

$$SINR_{opt} = \frac{|y_t|^2}{|y_u|^2} = \frac{\xi_t |\mathbf{w}_{opt}^H \mathbf{e}|^2}{\mathbf{w}_{opt}^H \mathbf{R}_u \mathbf{w}_{opt}} = \frac{\xi_t |\mathbf{w}_{opt}^H \mathbf{e}|^2}{|\mathbf{w}_{opt}^H \mathbf{e}|} \quad (8)$$

where $\xi_t = E\{|\alpha|^2\}$.

For an unknown signal amplitude, a detection test statistic (DTS) of STAP has been proposed as the ratio of the output power to the power of interference and noise (Robey, et al, 1992),

$$\Lambda_{STAP} = \frac{|\mathbf{w}_{opt}^H \mathbf{x}|^2}{\mathbf{w}_{opt}^H \mathbf{R}_u \mathbf{w}_{opt}} = \frac{|\mathbf{w}_{opt}^H \mathbf{x}|^2}{|\mathbf{w}_{opt}^H \mathbf{e}|} \quad (9)$$

Comparing (8) and (9) we can see that the STAP DTS is actually the SINR of the signal \mathbf{x} . In operations, once Λ_{STAP} exceeds a threshold, target presence is declared.

3. Classical Displaced Phase Centre Antenna

3.1 Displaced Phase Centre Antenna

DPCA processing is a technique for countering the platform motion induced clutter spectrum spreading. The basic concept is to make the antenna appear stationary even though the platform is moving forward by electronically shifting the receive aperture backwards during the operation (Morris and Harkness, 1996).

An airborne linear equispaced phased array antenna aligned with the flight direction and looking in the broadside direction is the default configuration in this report (though the radar is allowed to steer its look direction off the broadside direction, see numerical examples in Section 5). In particular, let a platform be moving in the x -direction, at a speed of v_a , a linear antenna array with N elements be parallel with the direction of motion, and looking at the broadside y -direction, as shown in Figure 1. Symbols H , R , θ and ϕ denote platform height, range, elevation angle and azimuth angle, respectively.

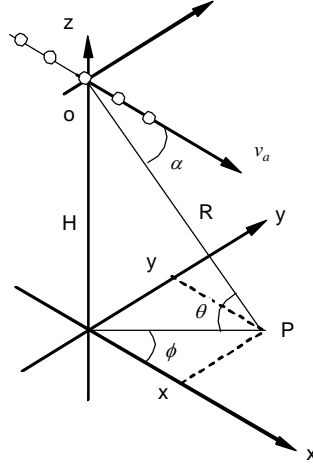


Figure 1: Geometry of a linear airborne antenna array.

With the common full-array transmit aperture, the clutter return from clutter patch P received by antenna element n for pulse m is (Ward, 1994),

$$c_{m,n} = (\sigma^2 \xi_P)^{1/2} \exp(j\varphi_P) \exp[j2\pi(n + 2v_a T_r m / d) \frac{d}{\lambda} \cos \theta \cos \phi] \quad (10)$$

where σ^2 is the thermal noise level of antenna, ξ_P is the single-pulse single-element clutter-to-noise ratio (CNR) for the clutter patch P , φ_P is a phase term induced by clutter patch P , T_r is the pulse repetition interval (PRI), d and λ are the antenna element space and radar frequency, respectively.

The DPCA condition for the above configuration requires the so-called clutter slope

$$\beta = 2v_a T_r / d \quad (11)$$

to be an integer. When $\beta = 1$, we have from (10),

$$c_{m+k,n-k} = c_{m,n} \quad k = 1, 2, \dots \quad (12)$$

It means that the phase centre of antenna element $n-k$ will move to the phase centre of antenna element n after k pulses as shown in Figure 2 (a). As a result the clutter signal received by element n from pulse m should be statistically equal to the clutter signal received by element $n-1$ from pulse $m+1$. The clutter cancellation can be achieved if we subtract them from each other. Having said so, it is worth noting that the nature of radar signals is a random process. The phase term φ_P and the intensity

term ξ_p are random variables and each obeys its own pdf. Equation (12) therefore should be understood as $E\{c_{m+k,n-k}\} = E\{c_{m,n}\}$, or $c_{m+k,n-k} - c_{m,n} = \delta_{m,n}(k)$ where $\delta_{m,n}(k)$ is a zero mean random variable.

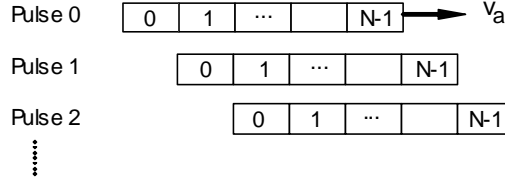


Figure 2: Effective array positions for successive pulses of a CPI with $\beta = 1$.

Equation (11) imposes serious limitations on any implementation of the DPCA technique. Once the element spacing and the pulse repetition frequency (PRF) are fixed, the platform velocity is also constrained. In practice, even if the condition of (11) is satisfied, the clutter cancellation is still limited due to other factors such as irregular motion and crabbing of the aircraft, spatial decorrelation among antenna elements and temporal decorrelation among pulses, as well as due to the intrinsic motion of clutter.

3.2 Blum's Adaptive DPCA

Adaptive processing can tolerate certain perturbations. It is thus natural to include adaptivity into DPCA processing to restore performance under non DPCA conditions. Blum et al (1996) first proposed a suboptimum technique (which is optimum if the number of pulses in a CPI is two) and called it adaptive DPCA. (Blum et al, 1996, Klemm, 2002, Chapter 7, Guerri, 2003, Chapter 5). The algorithm was further discussed and expressed in a more general form by Guerri (2003, Chapter 5).

To derive the Blum ADPCA, let us start from the case of a two-pulse system. According to STAP (1), the optimum weighting vector is,

$$\mathbf{w}_{opt} = \mathbf{R}_{0:1}^{-1} \begin{bmatrix} \mathbf{e}(0) \\ \mathbf{e}(1) \end{bmatrix} \quad (13)$$

where $\mathbf{R}_{0:1} \in \mathbb{C}^{2N \times 2N}$ is the covariance matrix of the undesired signals corresponding to pulses 0 and 1. Vectors $\mathbf{e}(0)$ and $\mathbf{e}(1) \in \mathbb{C}^{N \times 1}$ are sub-spatial-temporal steering vectors also corresponding to pulses 0 and 1, respectively, whose explicit expression is given in (6). This two-pulse processor formed from the principle of STAP is called two-pulse ADPCA by Blum et al (1996). It can be seen that the Blum ADPCA processor is the same as the STAP processor and thus optimum. If the number of pulses is greater

than two, each pair of pulses forms a two-pulse canceller; overall the weighting vector of the Blum ADPCA is (Blum et al, 1996, Guerri, 2003),

$$\mathbf{w}_{ADPCA} = \begin{bmatrix} \mathbf{R}_{0:1}^{-1} & \mathbf{0} & \mathbf{0} & \mathbf{0} \\ \mathbf{0} & \mathbf{R}_{1:2}^{-1} & \mathbf{0} & \mathbf{0} \\ \mathbf{0} & \mathbf{0} & \ddots & \mathbf{0} \\ \mathbf{0} & \mathbf{0} & \mathbf{0} & \mathbf{R}_{(M-2):(M-1)}^{-1} \end{bmatrix} \begin{bmatrix} \mathbf{e}(0:1) \\ \mathbf{e}(1:2) \\ \vdots \\ \mathbf{e}(M-2:M-1) \end{bmatrix} \quad (14)$$

where $\mathbf{R}_{m:m+1} \in \mathbb{C}^{2N \times 2N}$ is the covariance matrix of the undesired signals and $\mathbf{e}(m:m+1) = \begin{bmatrix} \mathbf{e}(m) \\ \mathbf{e}(m+1) \end{bmatrix}$ the spatial-temporal steering vector corresponding to pulses m and $m+1$, for $m = 0, 2, \dots, M-2$.

Equation (14) can be expressed as,

$$\mathbf{w}_{ADPCA} = \begin{bmatrix} \mathbf{R}_{0:1} & \mathbf{0} & \mathbf{0} & \mathbf{0} \\ \mathbf{0} & \mathbf{R}_{1:2} & \mathbf{0} & \mathbf{0} \\ \mathbf{0} & \mathbf{0} & \ddots & \mathbf{0} \\ \mathbf{0} & \mathbf{0} & \mathbf{0} & \mathbf{R}_{(M-2):(M-1)} \end{bmatrix}^{-1} \mathbf{\Gamma} \mathbf{e} \quad (15)$$

where

$$\mathbf{\Gamma} = \begin{bmatrix} {}_0\mathbf{I}_{2N \times 2N} & \mathbf{0}_{2N \times N} & \cdots & \mathbf{0}_{2N \times N} \\ \mathbf{0}_{2N \times N} & {}_1\mathbf{I}_{2N \times 2N} & \cdots & \mathbf{0}_{2N \times N} \\ \vdots & & \ddots & \\ \mathbf{0}_{2N \times N} & \mathbf{0}_{2N \times N} & \cdots & {}_{M-2}\mathbf{I}_{2N \times 2N} \end{bmatrix} \quad (16)$$

where $\mathbf{I}_{2N \times 2N}$ is a $2N \times 2N$ identity matrix, $\mathbf{0}_{2N \times N}$ a $2N \times N$ zero matrix, and

$$\mathbf{e} = \begin{bmatrix} \mathbf{e}(0) \\ \mathbf{e}(1) \\ \vdots \\ \mathbf{e}(M-1) \end{bmatrix} \quad (17)$$

is the original steering vector.

The corresponding test statistic is,

$$\Lambda = \frac{|\mathbf{w}_{ADPCA}^H \mathbf{x}_\Gamma|^2}{\mathbf{w}_{ADPCA}^H \mathbf{R}_\Gamma \mathbf{w}_{ADPCA}} \quad (18)$$

where $\mathbf{x}_\Gamma = \mathbf{\Gamma} \mathbf{x}$ and $\mathbf{R}_\Gamma = \mathbf{\Gamma} \mathbf{R}_u \mathbf{\Gamma}^H$. If Λ exceeds a threshold, target presence is declared. It should be pointed out that because $\mathbf{w}_{ADPCA} \neq \mathbf{R}_\Gamma^{-1} \mathbf{\Gamma} \mathbf{e}$ (\mathbf{R}_Γ^{-1} does not exist, see below), the denominator of (18) cannot be further simplified as in (9).

The above Blum ADPCA processor (15) can be considered as a linear transform, $\mathbf{\Gamma}$, of the original vector space, i.e., the signal snapshot \mathbf{x} becomes $\mathbf{\Gamma} \mathbf{x}$ and the spatial-temporal steering vector \mathbf{e} becomes $\mathbf{\Gamma} \mathbf{e}$. However,

$$\begin{bmatrix} \mathbf{R}_{0:1} & \mathbf{0} & \mathbf{0} & \mathbf{0} \\ \mathbf{0} & \mathbf{R}_{1:2} & \mathbf{0} & \mathbf{0} \\ \mathbf{0} & \mathbf{0} & \ddots & \mathbf{0} \\ \mathbf{0} & \mathbf{0} & \mathbf{0} & \mathbf{R}_{(M-2):(M-1)} \end{bmatrix} \neq E\{(\mathbf{\Gamma} \mathbf{x})(\mathbf{\Gamma} \mathbf{x})^H\} = E\{\mathbf{x}_\Gamma \mathbf{x}_\Gamma^H\} = \mathbf{\Gamma} \mathbf{R}_u \mathbf{\Gamma}^H \quad \text{if } M > 2 \quad (19)$$

Therefore, the Blum ADPCA is not optimal except for $M = 2$.

The non-equal sign of (19) is easy to prove. One method is given here. The rank of the matrix on the left side of the non-equal sign is $2N(M-1)$ as each sub-matrix is a full rank $2N \times 2N$ matrix. Because \mathbf{R}_u is a positive-definite Hermitian matrix, the rank of the matrix product on the right side of the non-equal sign is $r(\mathbf{\Gamma} \mathbf{R}_u \mathbf{\Gamma}^H) = r((\mathbf{\Gamma} \mathbf{R}_u^{1/2})(\mathbf{\Gamma} \mathbf{R}_u^{1/2})^H) = r(\mathbf{\Gamma} \mathbf{R}_u^{1/2}) = \min\{r(\mathbf{\Gamma}), r(\mathbf{R}_u^{1/2})\} = MN$, where $r(\cdot)$ is the rank function. This proof also shows that there does not exist a general linear transform $\mathbf{\Gamma}$ which lets the equal sign hold except for the case of $M = 2$. The proof also indicates the flaw in some equations given by Guerci (2003, Chapter 5).

To illustrate the above, we demonstrate here an explicit example of $N = 2$ and $M = 3$. The snapshot vector and the transform matrix, respectively, are,

$$\mathbf{x} = \begin{bmatrix} x_{00} \\ x_{01} \\ x_{10} \\ x_{11} \\ x_{20} \\ x_{21} \end{bmatrix} \quad \text{and} \quad \mathbf{\Gamma} = \begin{bmatrix} 1 & 0 & 0 & 0 & 0 & 0 \\ 0 & 1 & 0 & 0 & 0 & 0 \\ 0 & 0 & 1 & 0 & 0 & 0 \\ 0 & 0 & 0 & 1 & 0 & 0 \\ 0 & 0 & 1 & 0 & 0 & 0 \\ 0 & 0 & 0 & 1 & 0 & 0 \\ 0 & 0 & 0 & 0 & 1 & 0 \\ 0 & 0 & 0 & 0 & 0 & 1 \end{bmatrix} \quad (20)$$

where x_{mn} is the echo received by antenna element n for pulse m . The transformed covariance matrix is,

$$E\{\mathbf{\Gamma}(\mathbf{x}\mathbf{x}^H)\mathbf{\Gamma}^H\} = E \left\{ \begin{bmatrix} |x_{00}|^2 & x_{00}x_{01}^* & x_{00}x_{10}^* & x_{00}x_{11}^* & x_{00}x_{10}^* & x_{00}x_{11}^* & x_{00}x_{20}^* & x_{00}x_{21}^* \\ & |x_{01}|^2 & x_{01}x_{10}^* & x_{01}x_{11}^* & x_{01}x_{10}^* & x_{01}x_{11}^* & x_{01}x_{20}^* & x_{01}x_{21}^* \\ & & |x_{10}|^2 & x_{10}x_{11}^* & x_{10}x_{10}^* & x_{10}x_{11}^* & x_{10}x_{20}^* & x_{10}x_{21}^* \\ & & & |x_{11}|^2 & x_{11}x_{10}^* & |x_{11}|^2 & x_{11}x_{20}^* & x_{11}x_{21}^* \\ & & & & |x_{10}|^2 & x_{10}x_{11}^* & x_{10}x_{20}^* & x_{10}x_{21}^* \\ & & & & & |x_{11}|^2 & x_{11}x_{20}^* & x_{11}x_{21}^* \\ & & & & & & |x_{20}|^2 & x_{20}x_{21}^* \\ & & & & & & & |x_{21}|^2 \end{bmatrix} \right\} \quad (21)$$

Since the covariance matrix is Hermitian, we omit the elements below the main diagonal in (21). Comparing (21) with (15), we can see that the Blum ADPCA assumes zero sub-matrices (the unshaded sub-matrices) for all the off-main diagonal block matrices. Therefore the Blum ADPCA is not optimal for $M > 2$. As a consequence, the processing could lead to a significant SINR loss if the target's Doppler is close to that of the mainlobe clutter. We leave the performance evaluation to Section 5.

4. Proposed Adaptive Displaced Phase Centre Antenna

4.1 Formulation of Proposed ADPCA

The starting point in the proposed ADPCA is to form the difference between the measurements of array elements 1 to $N-1$ for pulse m and array elements 0 to $N-2$ for pulse $m+1$, as

$$\Delta \mathbf{x}(m) = \begin{bmatrix} \Delta x_{m,0} \\ \Delta x_{m,1} \\ \vdots \\ \Delta x_{m,N-2} \end{bmatrix} = \begin{bmatrix} x_{m,1} \\ x_{m,2} \\ \vdots \\ x_{m,N-1} \end{bmatrix} - \begin{bmatrix} x_{m+1,0} \\ x_{m+1,1} \\ \vdots \\ x_{m+1,N-2} \end{bmatrix} \quad (22)$$

which can be written in a compact form as,

$$\Delta \mathbf{x}(m) = [\mathbf{0} \quad \mathbf{I}_{N-1}] \mathbf{x}(m) - [\mathbf{I}_{N-1} \quad \mathbf{0}] \mathbf{x}(m+1) \quad m = 0, 1, \dots, M-2 \quad (23)$$

where $\mathbf{0} \in \mathbb{R}^{(N-1) \times 1}$ is a zero vector, $\mathbf{I}_{N-1} \in \mathbb{R}^{(N-1) \times (N-1)}$ is an identity matrix and $\Delta \mathbf{x}(m) \in \mathbb{C}^{(N-1) \times 1}$.

If the condition $\beta = 1$ is satisfied and there are no decorrelation effects, statistically all the clutter signals will be suppressed and $\Delta \mathbf{x}(m)$ given in (23) will only contain noise residue. If $\beta \neq 1$, which is the condition we are interest in, and/or there exist decorrelation effects, the clutter signal will only be partially cancelled. We modify (23) as,

$$\Delta \mathbf{x}(m) = [\mathbf{0} \quad \mathbf{I}_{N-1}] \mathbf{x}(m) - [\mathbf{A}(m) \quad \mathbf{0}] \mathbf{x}(m+1) \quad m = 0, 1, \dots, M-2 \quad (24)$$

where $\mathbf{A}(m) \in \mathbb{C}^{(N-1) \times (N-1)}$ is a parameter matrix to be determined. It means that instead of using a single measurement $x_{m+1,n-1}$ to estimate $x_{m,n}$ as in (23), we now using a linear combination of $x_{m+1,1}, \dots, x_{m+1,N-2}$. This is sometimes referred to as an autoregressive (AR) process (Marple, Jr, 1987) or PAMF (Roman et al, 2000, Michels et al, 2003, Rangaswamy and Michels, 1997).

Our goal is to maximally suppress the clutter, i.e., to minimise the mean residue power with respect to the parameter matrix $\mathbf{A}(m)$,

$$\min_{\mathbf{A}(m)} E\{\Delta \mathbf{x}^H(m) \Delta \mathbf{x}(m)\} \quad (25)$$

The optimal parameter matrix $\mathbf{A}(m)$ may be found from the least squares method (the Lagrange method),

$$\frac{\partial (E\{\Delta \mathbf{x}^H(m) \Delta \mathbf{x}(m)\})}{\partial \mathbf{A}(m)} = \mathbf{0} \quad (26)$$

Since $\mathbf{A}(m)$ in (25) is independent of the expectation operation, the expectation operation and the differentiation are interchangeable, and hence (26) can be expressed as,

$$E\left\{\frac{\partial (\Delta \mathbf{x}^H(m) \Delta \mathbf{x}(m))}{\partial \mathbf{A}(m)}\right\} = \mathbf{0} \quad (27)$$

The derivative of a scalar function $f(\mathbf{Q}) \in \mathbb{C}^{1 \times 1}$ with respect to $\mathbf{Q} \in \mathbb{C}^{m \times n}$ is an $m \times n$ matrix (Van Trees, 2002, p. 1399),

$$\frac{\partial}{\partial \mathbf{Q}} f(\mathbf{Q}) = \begin{bmatrix} \partial f / \partial q_{11} & \cdots & \partial f / \partial q_{1n} \\ & \ddots & \\ \partial f / \partial q_{m1} & & \partial f / \partial q_{mn} \end{bmatrix} \quad (28)$$

where q_{ik} , $i=1, \dots, m$, $k=1, \dots, n$, is the element of \mathbf{Q} . After tedious but straightforward algebra, the equation satisfying $E\left\{\frac{\partial (\Delta \mathbf{x}^H(m) \Delta \mathbf{x}(m))}{\partial \mathbf{A}(m)}\right\} = \mathbf{0}$ is,

$$\begin{aligned} \mathbf{A}^H(m) &= \begin{bmatrix} E\{|x_{m+1,0}|^2\} & \cdots & E\{x_{m+1,0} x_{m+1,N-2}^*\} \\ \vdots & \ddots & \vdots \\ E\{x_{m+1,N-2} x_{m+1,0}^*\} & \cdots & E\{|x_{m+1,N-2}|^2\} \end{bmatrix}^{-1} \begin{bmatrix} E\{x_{m+1,0} x_{m,1}^*\} & \cdots & E\{x_{m+1,0} x_{m,N-1}^*\} \\ \vdots & \ddots & \vdots \\ E\{x_{m+1,N-2} x_{m,1}^*\} & \cdots & E\{x_{m+1,N-2} x_{m,N-1}^*\} \end{bmatrix} \\ &= [\mathbf{R}_{m+1,m+1}(0:N-2, 0:N-2)]^{-1} \mathbf{R}_{m+1,m}(0:N-2, 1:N-1) \\ &\quad m = 0, 1, \dots, M-2 \end{aligned} \quad (29)$$

where $\mathbf{R}_{m,n}(m_1:m_2, n_1:n_2) \in \mathbb{C}^{(N-1) \times (N-1)}$ is a block submatrix of the covariance matrix \mathbf{R}_u . Subscripts m and n indicate the row and column of the block submatrix of \mathbf{R}_u ,

and the ranges in the brackets indicate the rows and columns of $\mathbf{R}_{m,n}$. The block matrix form of \mathbf{R}_u is given by,

$$\mathbf{R}_u = \begin{bmatrix} \mathbf{R}_{0,0} & \cdots & \mathbf{R}_{0,M-1} \\ \vdots & \ddots & \vdots \\ \mathbf{R}_{M-1,0} & \cdots & \mathbf{R}_{M-1,M-1} \end{bmatrix} \quad (30)$$

where $\mathbf{R}_{m,n} \in \mathbb{C}^{N \times N}$, $m, n = 0, \dots, M-1$.

For simplicity, we rewrite (29) as,

$$\mathbf{A}^H(m) = [\mathbf{R}'_{m+1,m+1}]^{-1} \mathbf{R}'_{m+1,m} \quad m = 0, \dots, M-2 \quad (31)$$

Since the true covariance matrix is unknown, $\mathbf{A}(m)$, $m = 0, \dots, M-2$, can only be estimated using sample data in practice. Assuming the radar system is well calibrated and stable, and the pulse train is uniform, then for fast calculation, we can assume $\mathbf{A}(m)$ to be independent of pulse number m in a CPI. This assumption allows the averaging processing to proceed using the slow-time (pulse) samples after the averaging processing using fast-time (range) samples, and has advantages and disadvantages. If there are sufficient data samples and each is an identically and independently distributed (iid) sample of undesired signal identical to that of CUT, then the averaging processing may lead to some processing gain loss as temporal correlation effects as well as differences are being averaged. On the other hand, if the data samples are limited, the averaging process should make the estimate of $\mathbf{A}(m)$ more accurate and result in a robust processor. Therefore, the assumption that $\mathbf{A}(m)$ is independent of m is not only for the reason of reducing calculation, but more importantly requires less sample data. The rationale of this assumption is given below. If clutter is modelled by the first-order clutter model, i.e., the model does not take account of various spatial and temporal decorrelation effects, the covariance matrix has a so-called Toeplitz-block-Toeplitz pattern (Ward, 1994), then we can immediately deduce all $\mathbf{A}(m)$, $m = 0, \dots, M-2$ to be identical. Temporal decorrelation effects such as range walk and clutter intrinsic motion are often modelled by the covariance matrix tapering (CMT) method which is often assumed stationary, i.e., the tapering coefficient is only a function of the interval between pulses (Guerci, 2003, Chapter 4, Clemm, 2002, Chapter 2). Under the CMT model assumption, $\mathbf{A}(m)$ is still independent of the pulses. Note also that this assumption does not require any specific spatial correlation form as the averaging process is only in the temporal domain, though most models of spatial correlation are also assumed stationary (Guerci, 2003, Chapter 4).

An averaging process in the slow-time domain results in the parameter matrix $\mathbf{A}(m)$ to be independent of pulses, as,

$$\mathbf{A}^H = \left[\frac{1}{M-1} \sum_{m=0}^{M-2} \mathbf{R}'_{m+1,m+1} \right]^{-1} \left[\frac{1}{M-1} \sum_{m=0}^{M-2} \mathbf{R}'_{m+1,m} \right] = \left[\sum_{m=0}^{M-2} \mathbf{R}'_{m+1,m+1} \right]^{-1} \left[\sum_{m=0}^{M-2} \mathbf{R}'_{m+1,m} \right] \quad (32)$$

The averaging process of (32) means that temporal correlations such as the effects of range walk and clutter intrinsic movement will be averaged (similar to the CMT models). We will give numerical comparisons in the next section to justify such a slow-time averaging process.

It is understood that if $\mathbf{A} = \mathbf{I}$, then the processor will reduce to the traditional DPCA with non-adaptability.

The transform from \mathbf{x} to $\Delta\mathbf{x}$ can be expressed in a compact form, as

$$\Delta\mathbf{x} = \mathbf{B}\mathbf{x} \quad (33)$$

where $\mathbf{B} \in \mathbb{C}^{(M-1)(N-1) \times MN}$ and has the form,

$$\mathbf{B} = \begin{bmatrix} \mathbf{0} & \mathbf{I} & -\mathbf{A} & \mathbf{0} & \mathbf{0} & \cdots & \mathbf{0} & \mathbf{0} \\ \mathbf{0} & \mathbf{0} & \mathbf{I} & -\mathbf{A} & \mathbf{0} & \cdots & \mathbf{0} & \mathbf{0} \\ \vdots & \vdots & \vdots & \ddots & \vdots & \vdots & \vdots & \vdots \\ \mathbf{0} & \mathbf{0} & \cdots & \cdots & \mathbf{0} & \mathbf{I} & -\mathbf{A} & \mathbf{0} \end{bmatrix} \quad (34)$$

We perform the same transform for the steering vector \mathbf{e} , as,

$$\mathbf{u} = \mathbf{B}\mathbf{e} \quad (35)$$

Analogous to STAP processing, for snapshot $\Delta\mathbf{x}$ and steering vector \mathbf{u} , the optimal weighting vector is,

$$\mathbf{w} = \gamma \mathbf{R}_{\Delta}^{-1} \mathbf{u} \quad (36)$$

where $\mathbf{R}_{\Delta} = E\{\Delta\mathbf{x}\Delta\mathbf{x}^H\}$ is the covariance matrix of the residue signal $\Delta\mathbf{x}$ and can be estimated using range samples, by

$$\hat{\mathbf{R}}_{\Delta} = \frac{1}{K} \sum_{k=1}^K \Delta\mathbf{x}_k \Delta\mathbf{x}_k^H = \mathbf{B} \hat{\mathbf{R}}_u \mathbf{B}^H \quad (37)$$

Since $\Delta\mathbf{x}$ is a residue noise vector, its elements should be mutually uncorrelated (the process of (33) is also referred to as a whitening process). The covariance matrix \mathbf{R}_{Δ}

therefore should only be a diagonal matrix, and its inverse is simply the inverse of each diagonal element. In reality, the non-diagonal elements of $\hat{\mathbf{R}}_{\Delta}$ may not be zero, but their values will be smaller compared to the diagonal elements, and the inverse can be found approximately by letting all non-diagonal elements equal zero, i.e.,

$$\tilde{\mathbf{R}}_{\Delta}^{-1} \approx [\text{diag}(\hat{\mathbf{R}}_{\Delta})]^{-1} \quad (38)$$

The corresponding weighting vector (36) becomes,

$$\tilde{\mathbf{w}} = \gamma \tilde{\mathbf{R}}_{\Delta}^{-1} \mathbf{u} \quad (39)$$

The weighting vector of (39) may not be optimal but should be close to the optimum.

The resultant test statistic is,

$$\Lambda_{ADPCA} = \frac{|\tilde{\mathbf{w}}^H \Delta \mathbf{x}|^2}{\tilde{\mathbf{w}}^H \hat{\mathbf{R}}_{\Delta} \tilde{\mathbf{w}}} \quad (40)$$

Since $\tilde{\mathbf{R}}_{\Delta}^{-1}$ is only an approximation of the inverse of $\hat{\mathbf{R}}_{\Delta}$, the denominator of (40) usually cannot be further simplified as has been done in (9).

4.2 Two Significant Advantages of Proposed ADPCA over STAP

There are two significant advantages of the proposed ADPCA over STAP, one is computational savings and the other is its robustness when reduced samples are used in parameter estimation.

4.2.1 Computational Savings

The computational savings can be readily estimated. In the estimation, we only count complex multiplication/division, and ignore addition/subtraction. For simplicity we also assume that no special digital signal processing (DSP) hardware is used, so that all calculations are treated with the same weight. Special structures of matrices such as complex conjugate symmetry, which often lead to special algorithms to save operational counts (ops), are also not considered. For instance, the number of ops for a matrix multiplication $\mathbf{Z} = \mathbf{X}\mathbf{Y}$ is lmn where $\mathbf{Z} \in \mathbb{C}^{m \times n}$, $\mathbf{X} \in \mathbb{C}^{m \times l}$ and $\mathbf{Y} \in \mathbb{C}^{l \times n}$.

To estimate the total ops required, we further assume that the fixed-window architecture is used in the process. The fixed-window architecture only uses a single covariance matrix estimated from a section of K range samples (secondary data) to process a section of K_{rg} range cells (primary data). In contrast, the sliding-window

architecture estimates the covariance matrix for each range cell (or a few cells) from its surrounding range cells. According to a previous study, the sliding-window processing does not show any noticeable SINR improvement compared to the fixed-window processing, though the former requires a much more considerable amount of computation (Dong, 2006).

Ops required for STAP and the proposed ADPCA algorithms are listed in Table 1 and Table 2, respectively. To easy understand, calculations are divided into 5 steps (c_1 to c_5) for STAP and 9 steps (d_1 to d_9) for the proposed ADPCA. Since the Doppler of the potential target signals is unknown, a search in Doppler frequency is necessary. In general we need at least M Doppler filters. The total ops required for processing K_{rg} range samples using the fixed window architecture for STAP is therefore,

$$c_t = c_1 + c_2 + M(c_3 + c_4) + K_{rg}Mc_5 \quad (41)$$

Similarly, the total ops required for processing K_{rg} range samples for the proposed ADPCA is,

$$d_t = d_1 + d_2 + d_3 + d_4 + M(d_5 + d_6 + d_7) + K_{rg}(d_8 + M d_9) \quad (42)$$

Table 1: Ops required for the STAP process.

| Algorithm | Task | Reference Eqn | Ops |
|---|---|---------------|-----------|
| c_1 - form \mathbf{R}_u using K range samples | $\hat{\mathbf{R}}_u = \frac{1}{K} \sum_{k=1}^K \mathbf{x}_k \mathbf{x}_k^H + \delta \mathbf{I}$ | (2) | $K(MN)^2$ |
| c_2 - compute \mathbf{R}_u^{-1} | $\hat{\mathbf{R}}_u^{-1}$ | (1) | $(MN)^3$ |
| c_3 - compute \mathbf{w}_{opt} | $\mathbf{w}_{opt} = \hat{\mathbf{R}}_u^{-1} \mathbf{e}$ | (1) | $(MN)^2$ |
| c_4 - compute Λ_{STAP0} | $\Lambda_{STAP0} = \mathbf{w}_{opt}^H \mathbf{R}_u \mathbf{w}_{opt}$ $= \mathbf{w}_{opt}^H \mathbf{e}$ | (9) | MN |
| c_5 - compute Λ_{STAP} | $\Lambda_{STAP} = \frac{ \mathbf{w}_{opt}^H \mathbf{x} ^2}{\Lambda_{STAP0}}$ | (9) | MN |

Table 2: Ops required for the proposed ADPCA process.

| Algorithm | Task | Reference Eqn | Ops |
|--|---|---------------|-------------------------|
| d_1 - form \mathbf{A} | $\mathbf{A}^H = \left[\sum_{m=0}^{M-2} \mathbf{R}'_{m+1,m+1} \right]^{-1} \left[\sum_{m=0}^{M-2} \mathbf{R}'_{m+1,m} \right]$ | (22) | $2M_A K N_A^2 + 2N_A^3$ |
| d_2 - form $K \Delta \mathbf{x}'s$ | $\Delta \mathbf{x} = \mathbf{B} \mathbf{x}$ | (23) | $K(M_A N_A^2)$ |
| d_3 - form \mathbf{R}_Δ | $\hat{\mathbf{R}}_\Delta = \frac{1}{K} \sum_{k=1}^K \Delta \mathbf{x}_k \Delta \mathbf{x}_k^H$ | (27) | $K(M_A N_A)^2$ |
| d_4 - compute \mathbf{R}_Δ^{-1} | $\tilde{\mathbf{R}}_\Delta^{-1} \approx [\text{diag}(\hat{\mathbf{R}}_\Delta)]^{-1}$ | (28) | $M_A N_A$ |
| d_5 - form \mathbf{u} | $\mathbf{u} = \mathbf{B} \mathbf{e}$ | (25) | $M_A N_A^2$ |
| d_6 - compute \mathbf{w} | $\tilde{\mathbf{w}} = \tilde{\mathbf{R}}_\Delta^{-1} \mathbf{u}$ | (29) | $M_A N_A$ |
| d_7 - Λ_{ADPCA0} | $\Lambda_{ADPCA0} = \tilde{\mathbf{w}}^H \hat{\mathbf{R}}_\Delta \tilde{\mathbf{w}}$ | (30) | $(M_A N_A)^2 + M_A N_A$ |
| d_8 - form $\Delta \mathbf{x}$ | $\Delta \mathbf{x} = \mathbf{B} \mathbf{x}$ | (23) | $M_A N_A^2$ |
| d_9 - Λ_{ADPCA} | $\Lambda_{ADPCA} = \frac{ \tilde{\mathbf{w}}^H \Delta \mathbf{x} ^2}{\Lambda_{ADPCA0}}$ | (30) | $M_A N_A$ |

Note: where $M_A = M - 1$ and $N_A = N - 1$.

Figure 3 shows the ratio of d_i / c_i in percentage, as a function of the number of pulses, M , with three given parameters, the number of antenna elements ($N = 20, 30, 50$), the number of range samples ($K = 100$) used for estimating the covariance matrix and the number of range cells ($K_{rg} = 500$) to be processed. The dominant part of the STAP algorithm lies in the computation of the inverse of the covariance matrix, which requires ops equal to the cube of the dimension of the matrix. On the other hand, the proposed ADPCA does not require the inversion of the full dimensional covariance matrix, so its ops are considerably less. In general, the proposed ADPCA algorithm only needs about 5-10% of the calculation required by the STAP algorithm. The larger the values of M and N , the smaller is the ratio of d_i / c_i .

Furthermore, as mentioned, the inversion of the covariance matrix dominates the calculation in STAP. The method of the complete Gauss-Jordan elimination is often used to numerically compute the inverse of a matrix (Isaacson and Keller, 1966). Since this process is not linear, it is difficult to construct dedicated DPS hardware or perform parallel computation to implement the Gauss-Jordan elimination. On the other hand, it

can be seen that the dominant processes for ADPCA are linear. A linear transform can be easily implemented using either general DPS hardware or parallel computation. In this sense, the proposed ADPCA processing should have an even bigger computational advantage than the simple ops estimation and comparison shown in Figure 3.

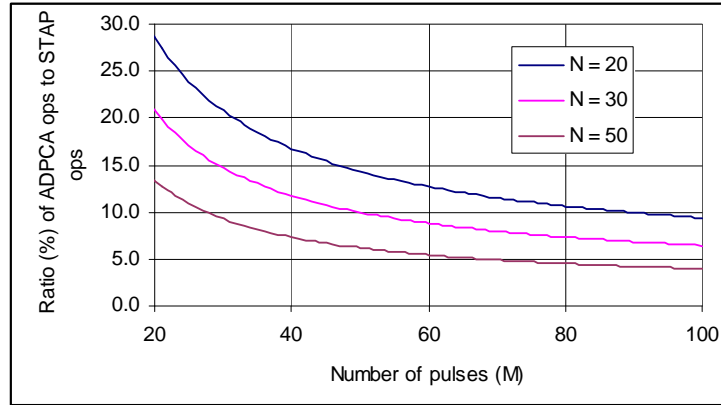


Figure 3: Ratio in percentage of the proposed ADPCA ops to the STAP ops with the parameters of $K = 100$ and $K_{rg} = 500$.

The ops required for the Blum ADPCA processor has not been calculated. Qualitatively its computational requirement is higher than that of the proposed ADPCA but much less than that of STAP. It will be seen later that the processor does not perform well, so its detection loss cannot be justified by its savings in computation requirements.

4.2.2 Robustness of Proposed ADPCA

The performance of any adaptive processor depends on an accurate estimation of its parameters. In STAP in order to accurately estimate the covariance matrix, twice as many iid range samples as the size of the covariance matrix itself are required (Reed et al, 1974, Ward, 1994), or more correctly, about twice the number of non-zero eigenvalues of the matrix¹. Since the size of the covariance matrix is MN , a significant number of range samples is required in order to guarantee a satisfactory performance of STAP. On the other hand, the proposed ADPCA uses a covariance matrix whose size is only $N-1$. This suggests that the number of range samples required for an accurate estimate of the parameter matrix should be significantly smaller than that for the estimate of the covariance matrix in STAP. A physical interpretation for the different requirement of the range samples is that STAP only utilises averaging processing in the fast-time domain (range samples) to estimate its parameters whereas the proposed ADPCA employs not only the fast-time but also the slow-time (pulse

¹Due to the existence of thermal noise, the non-zero eigenvalue means that the eigenvalue is greater than the mean power of the thermal noise.

samples) averaging processing to estimate its parameters. Therefore, in the case of reduced samples, STAP may not perform due to a poor estimate of the covariance matrix while the ADPCA still robustly performs. More detailed analysis is given through examples in the next section.

4.2.3 Inherent SINR Loss of ADPCA

We need to point out that the proposed ADPCA is a dimensionality-loss process. Both the number of effective antenna elements and the number of effective pulses in a CPI are reduced by one. Therefore theoretically the maximum coherent processing gain it can achieve is $10\log_{10}[(N-1)(M-1)]$ dB compared to the gain of $10\log_{10}(NM)$ dB for STAP.

5. Performance Assessment

A dataset generated using the high fidelity airborne radar simulation software, RLSTAP, and a dataset collected by the MCARM system were used to test the performance of the proposed ADPCA. The results of the Blum ADPCA were also computed, so the significant improvement of the proposed processor can be appreciated. The results of STAP serve as test benchmarks as they are optimum.

5.1 RLSTAP Dataset

Table 3 and Table 4 list parameters of the radar, platform and targets used in generating the simulated dataset. RLSTAP calculates clutter returns based on the United States Geological Survey Land Use Land Cover (USGS LULC) data and the Digital Terrain Elevation (DTE) data. Figure 4 shows the LULC data superposed onto the DTE data for the Washington D.C. area with the radar beam pattern. Details of the clutter model used in RLSTAP are unknown.

Table 3: Parameters used in RLSTAP for generating the simulated airborne radar dataset.

| Parameter | Specification |
|--------------------------|--|
| Radar | |
| Phased array | Linear 20-by-4 elements, element pattern $\cos^{0.6}(\phi)$, azimuth spacing 0.12m, elevation spacing 0.15m uniform tapering for transmit |
| Carrier frequency | 1.2 GHz |
| Polarisation | VV |
| LFM bandwidth | 2 MHz |
| PRF | 2 KHz |
| Number of pulses per CPI | 32 |
| Peak power | 30kW |
| Duty | 10% |
| Sample interval | 0.2 μ s |
| Look direction | 30° from broadside towards nose, horizontal |
| Platform | |
| Height | 7 km |
| Speed | 175 m/s |
| Undesired Signals | |
| Thermal noise | Gaussian |
| Clutter | Washington D. C. area: (38.1°N, -76.9°E) to (39.6°N, -- 75.2°E) |
| Jamming | None |

Table 4: Parameters of targets.

| Parameters | Target 1 | Target 2 | Target 3 |
|---------------------------------|------------|--------------|----------|
| Height (km) | 3 | 3 | 3 |
| Position off mainlobe direction | 1 km north | 0.5 km south | 0 |
| Radial velocity (m/s) | -100 | -20 | 150 |
| Doppler frequency (Hz) | -500 | 860* | -500 |
| Range (km) | 50 | 60 | 70 |
| Range bin Number | 1948 | 2256 | 2598 |
| RCS (sqm) | 1 | 1 | 1 |

*Since the radar looks at 30° from broadside towards the nose, the main lobe clutter has a Doppler frequency of 700 Hz. Therefore, target 2 is the most difficult to detect as its Doppler frequency is close to that of the mainlobe clutter.

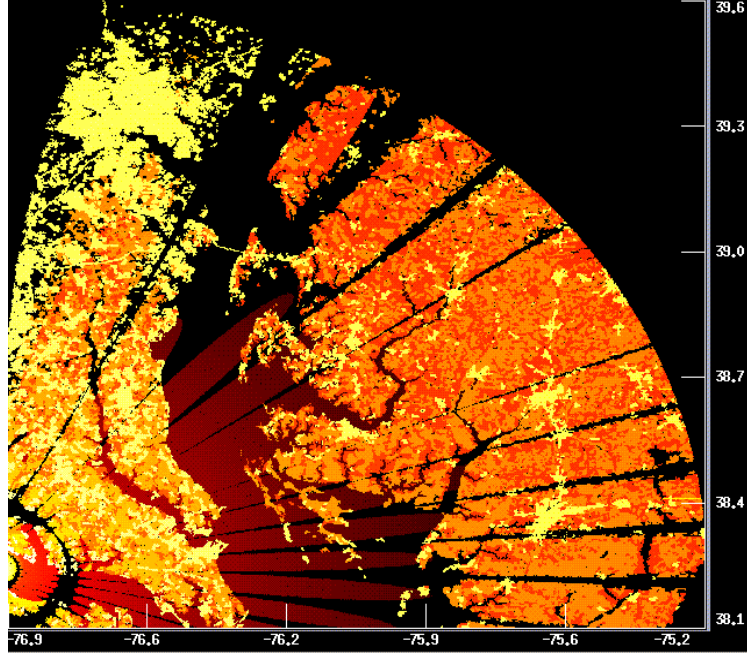


Figure 4: The LULC data superposed on the DTE data of the Washington D. C. area.

Before showing the results, it is worth noting that

- Due to the effect of the clutter foldover, clutter returns from the first pulse statistically differ from those collected from the following pulses. The data collected by the first pulse was therefore discarded in the calculation. The number of pulses in a CPI and the number of antenna elements in the azimuth actually used in the calculation are $M = 31$ and $N = 20$, respectively.
- According to the parameters given in Table 3, $\beta = 1.46$ so the simulation was under a non-DPCA condition.
- The range resolution of the system is $\Delta r = c/(2B)$ where c is the speed of light and B the bandwidth of the LFM. The corresponding range sampling interval for iid samples should be $\Delta t = 1/B = 0.5 \mu s$. The actual range sampling interval used in RLSTAP was $0.2 \mu s$. Therefore, the consecutive range samples will not be iid. Theoretically every third, or greater, samples should be iid samples.
- The DL-SMI method (Carlson, 1988) was used in the STAP analysis. The diagonally loaded coefficient was set to be 50dB below the mean value of the diagonal elements of the covariance matrix. This diagonal loading means that the single-pulse single-element CNR is no better than 50dB (the single-pulse single-element CNR for the simulation was unknown but could be computed from the data).
- Hamming windows were used for both the spatial and temporal steering vectors $\mathbf{e}(f_{ts})$ and $\mathbf{e}(f_{td})$ in the processing.

Figure 5 and Figure 6 compare the results of the STAP, DPCA (non-adaptability), Blum's ADPCA and the proposed ADPCA obtained from using 267 non-consecutive range samples with an interval of 3 $(801:3:1600)^2$. Figure 5 shows the signal level as a function of both the range bin and Doppler bin, whereas Figure 6 is a view of Figure 5 from the direction perpendicular to the range bin, i.e., the Doppler bins are collapsed onto the range. It was found that STAP produced the best result if sufficient range samples were used in forming the covariance matrix. It can be seen that there is a few dB signal loss for target 2 (the mid range one, that is the most difficult to be detected, see the note on Table 4) in the results of both ADPCA processors (the loss of the Blum ADPCA is higher though) compared to the result of STAP, which can be clearly viewed from Figure 6. This is not a surprise result, as STAP is optimal if the covariance matrix is accurately estimated. The DPCA with non-adaptability processor performs poorly as expected since the radar was operated under a non-DPCA condition. Further numerical examples will not include this DPCA processor.

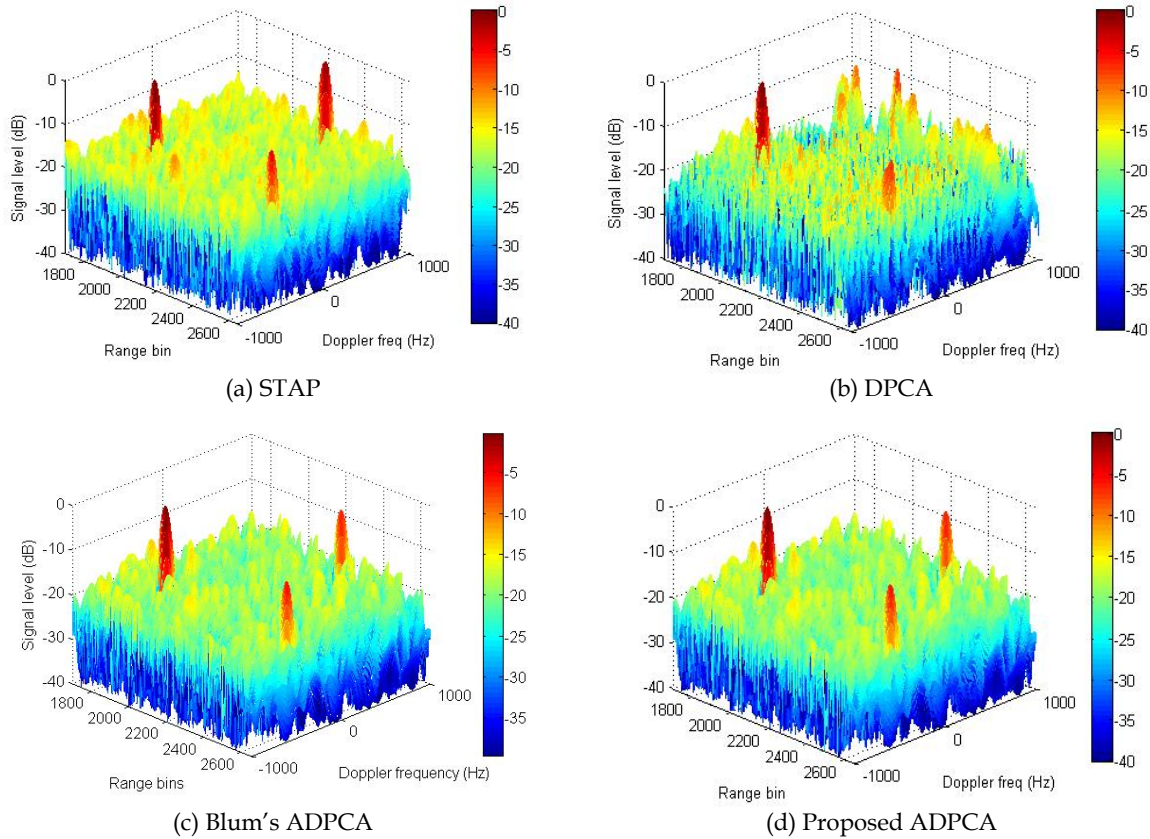


Figure 5: Performance comparison between (a) STAP, (b) DPCA, (c) Blum's ADPCA and (d) proposed ADPCA for the RLSTAP data using 267 range samples in forming the covariance matrix.

²The use of 800 $(801:1600)$ consecutive range samples gave a very similar result.

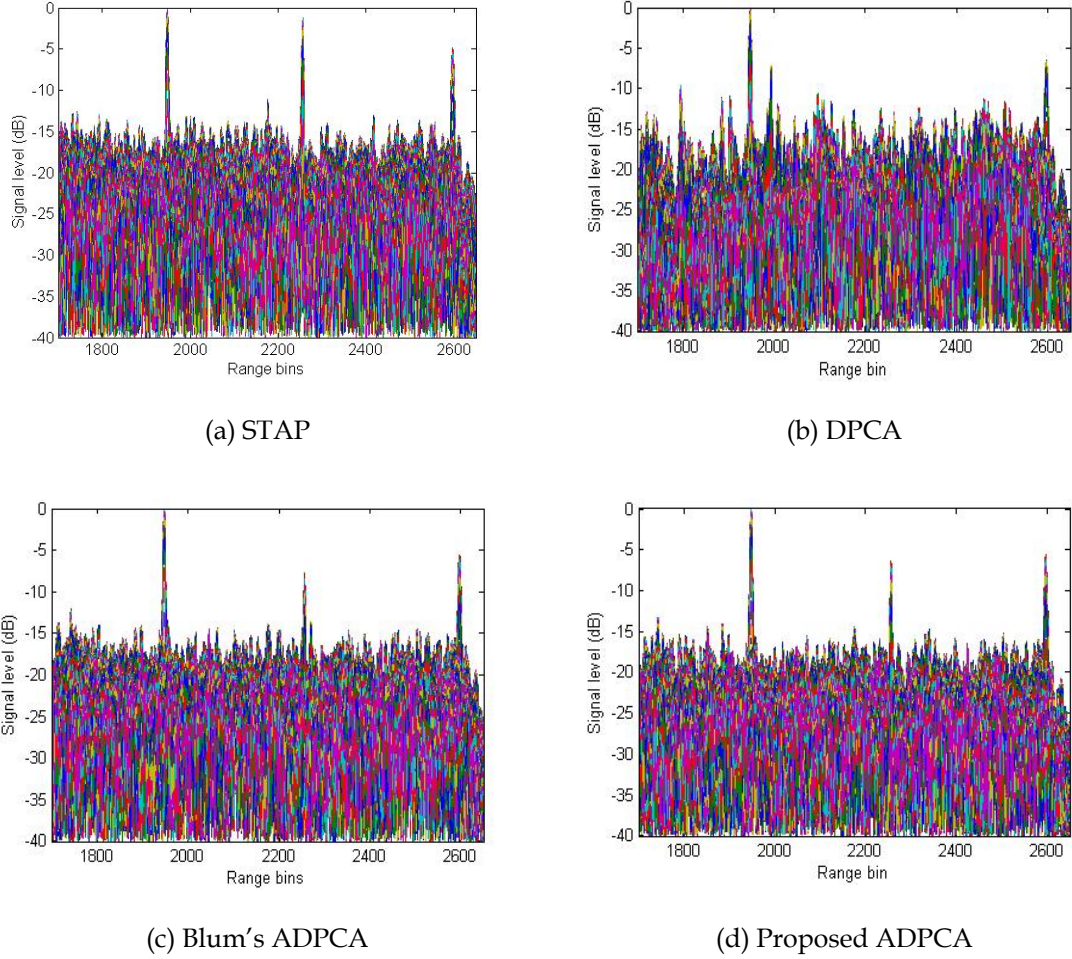


Figure 6: Performance comparison between (a) STAP, (b) DPCA, (c) Blum's ADPCA and (d) proposed ADPCA for the RLSTAP data using 267 range samples in forming the covariance matrix. The results are plotted in the signal level versus range with the Doppler bins collapsed onto the range.

Reducing the number of range samples for estimation of the covariance matrix leads to quite different results. Figure 7 and Figure 8 compare the results of STAP and the two ADPCA algorithms using 100 non-consecutive range samples (1301:3:1600). It can be seen that the clutter level has lifted significantly for the STAP due to insufficient range samples used for estimating the covariance matrix. Target 2 becomes hardly detectable for the Blum ADPCA. The performance of the proposed ADPCA, however, remains almost unchanged.

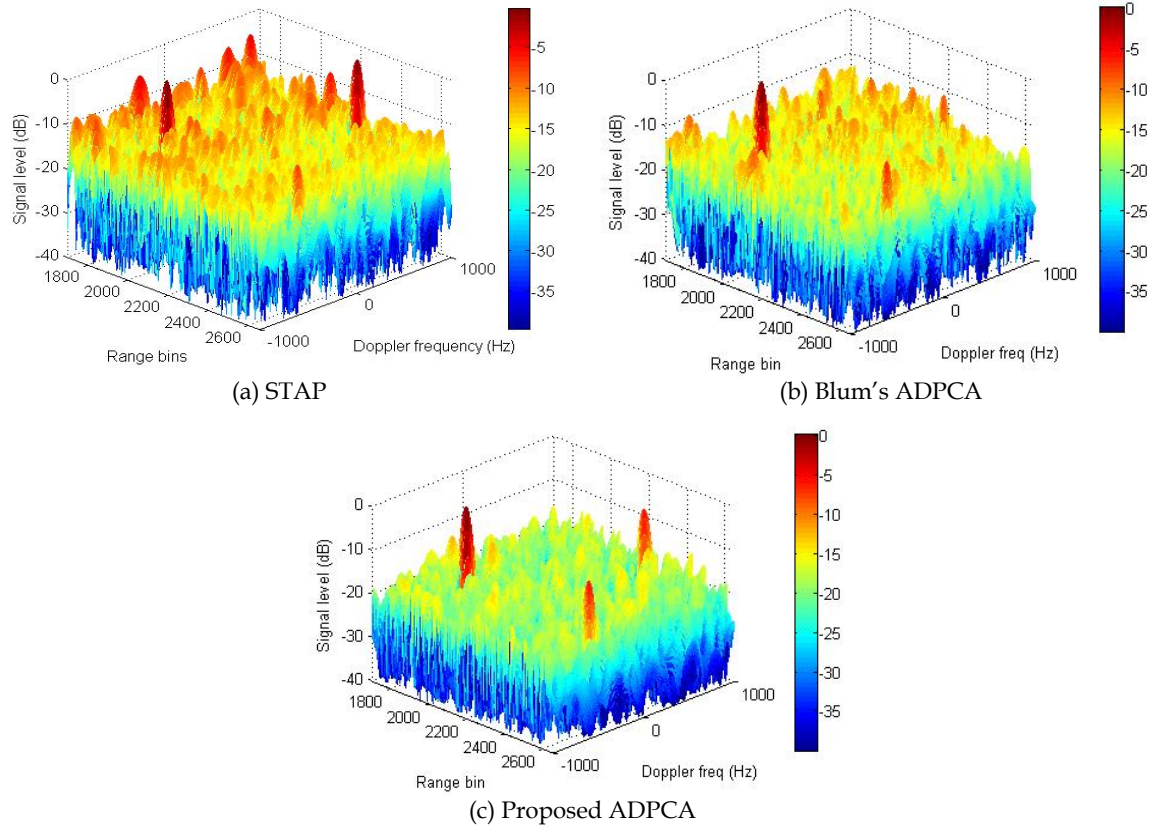


Figure 7: Performance comparison between (a) STAP, (b) Blum's ADPCA and (c) proposed ADPCA for the RLSTAP data using 100 range samples in forming the covariance matrix.

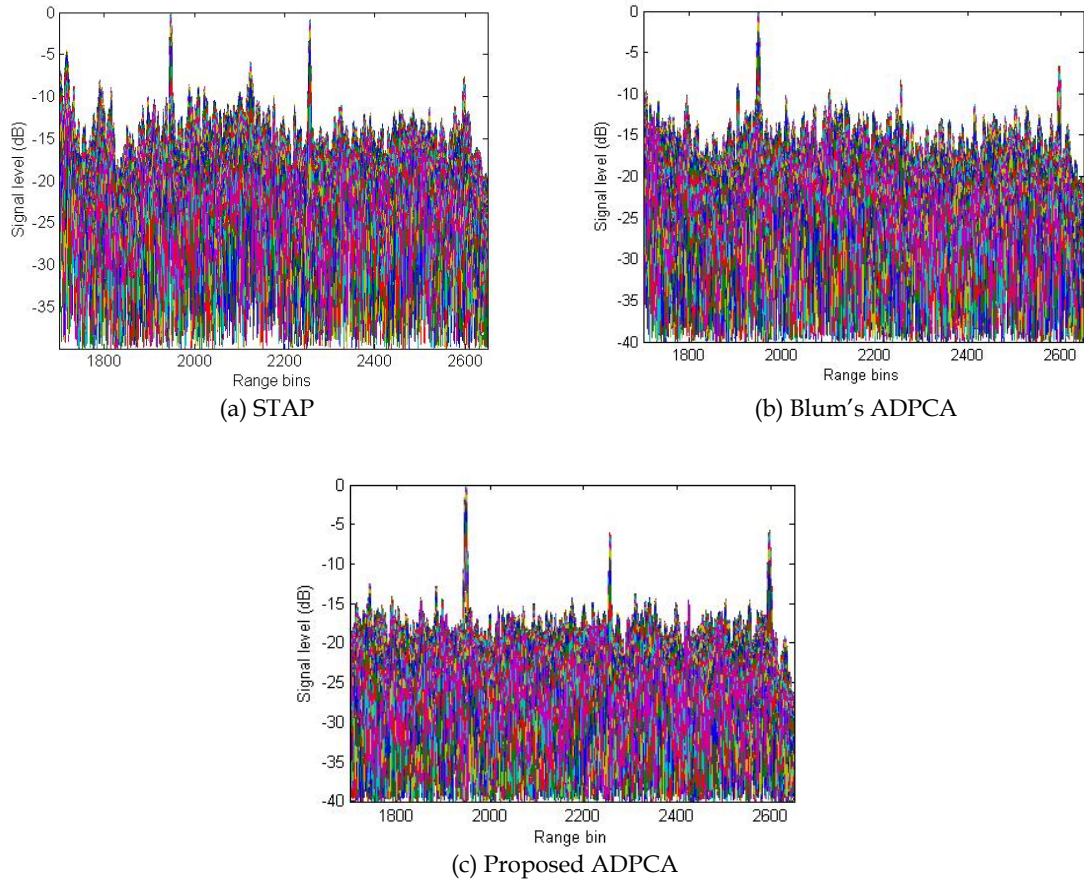


Figure 8: Performance comparison between (a) STAP, (b) Blum's ADPCA and (c) proposed ADPCA for the RLSTAP data using 100 range samples in forming the covariance matrix. The results are plotted in signal level versus range with the Doppler bins collapsed onto the range.

An example with a further reduction in range samples is shown in Figure 9 and Figure 10 in which only 50 (1451:3:1600) non-consecutive range samples were used in estimating the covariance matrix. It can be seen that for such a small number of range samples both STAP and Blum's ADPCA stop performing, whereas the proposed ADPCA still robustly works with little degradation.

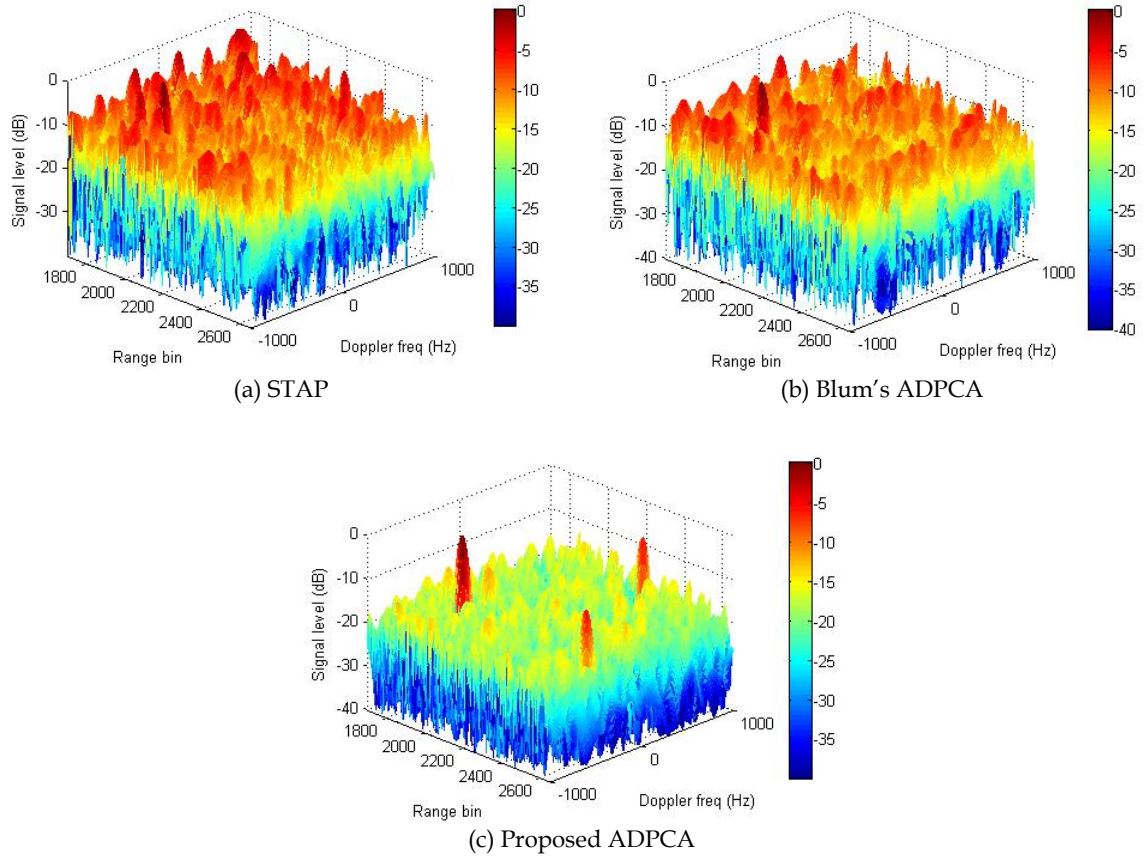


Figure 9: Performance comparison between (a) STAP, (b) Blum's ADPCA and (c) proposed ADPCA for the RLSTAP data using 50 range samples in forming the covariance matrix.

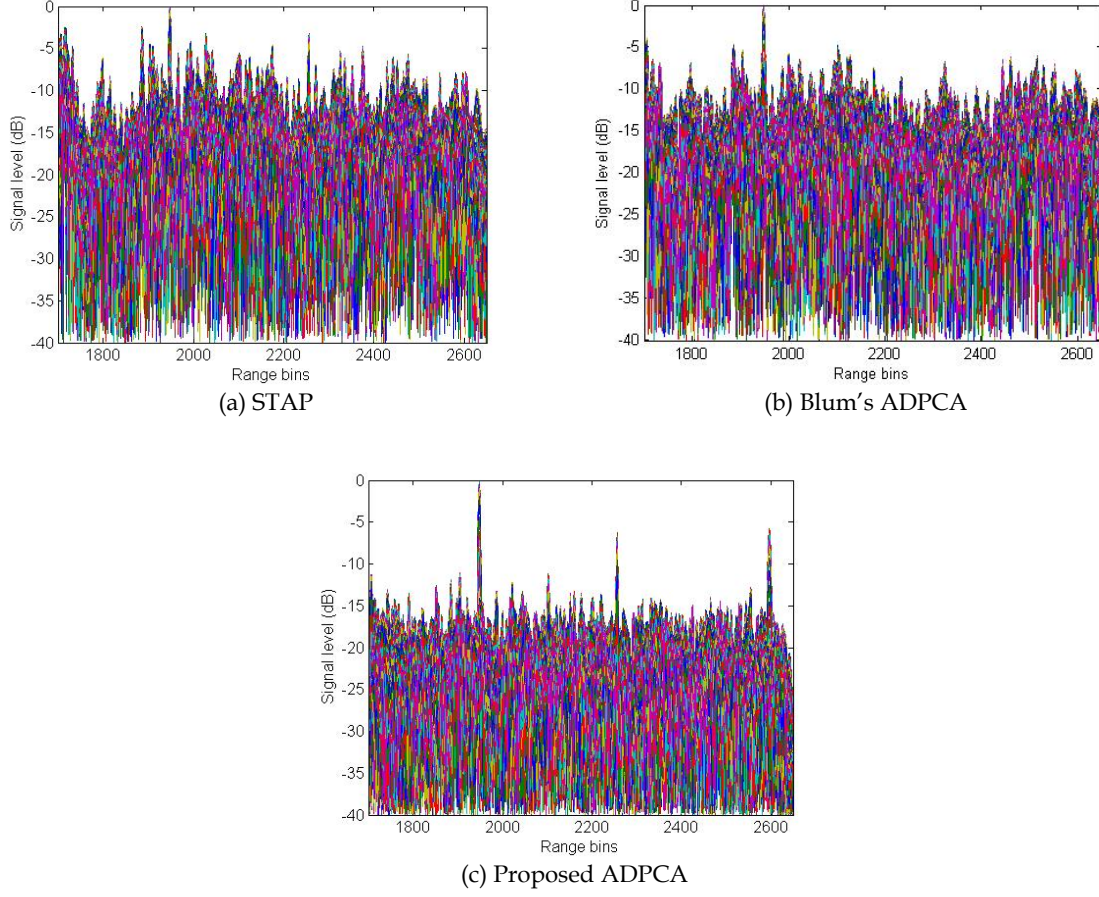


Figure 10: Performance comparison between (a) STAP, (b) Blum's ADPCA and (c) proposed ADPCA for the RLSTAP data using 50 range samples in forming the covariance matrix. The results are plotted in the signal level versus range with the Doppler bins collapsed onto the range.

In Section 4 we discussed the advantages and disadvantages of the averaging processing in the slow-time domain. In order to see the effect of this process especially with a reduced number of range samples, we show in Figure 11 the results of the proposed ADPCA without slow-time averaging, i.e., $\mathbf{A}(m)$, $m = 0, \dots, M - 2$ are calculated individually using (31). Range samples used are the same as those of Figure 5, Figure 7 and Figure 9, respectively. It can be seen that the averaging processing helps significantly for the case of reduced range samples.

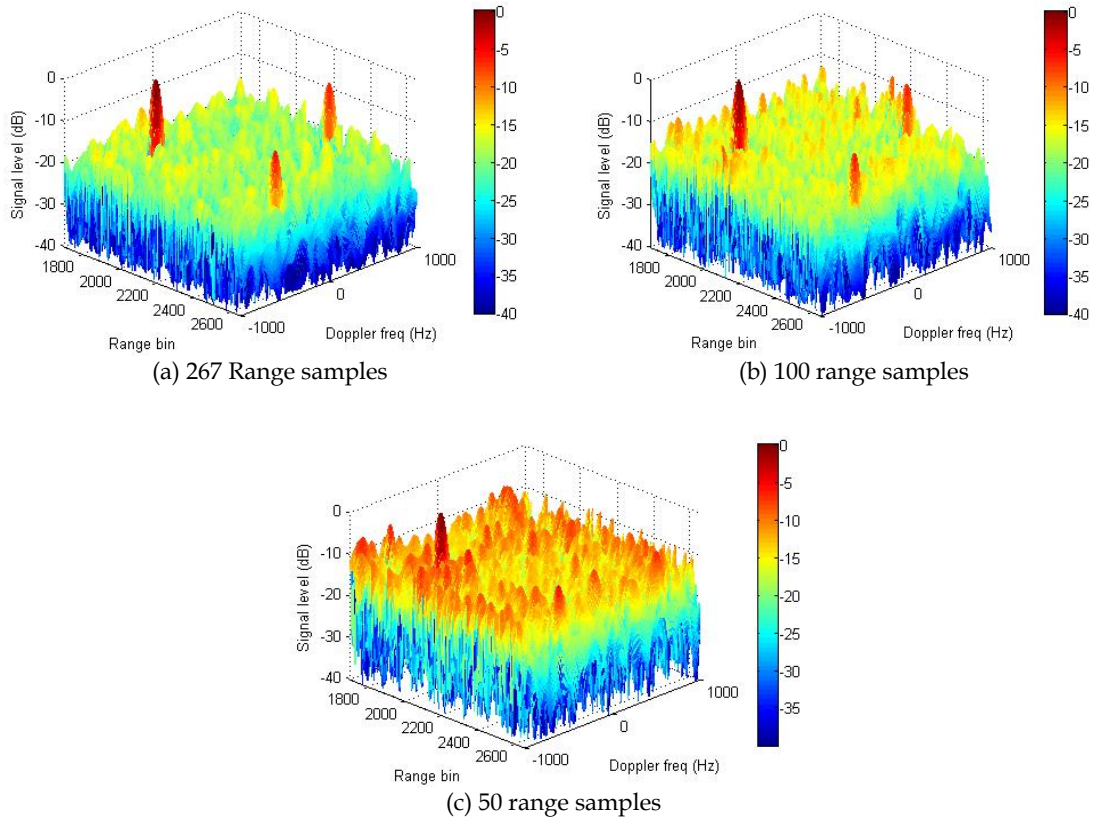


Figure 11: Results of the proposed ADPCA without using slow-time averaging processing.

It is known that in order to accurately estimate the covariance matrix, the number of samples required is twice the dimension of the covariance matrix itself (Reed et al, 1974, Ward, 1994), or more correctly, about twice the number of non-zero eigenvalues of the matrix (see footnote 1). Figure 12 shows the eigenvalues of the covariance matrix in descending order (the matrix itself was formed using 800 consecutive range samples (800:1600) with a diagonal loading of 50dB below the mean value of the diagonal elements of the covariance matrix). The number of eigenvalues above the noise level is about 200. Therefore, theoretically STAP requires about 400 iid range samples in order to accurately estimate the covariance matrix, or about 250 iid range samples if we treat those eigenvalues that are 60dB below the maximum eigenvalue to be noise.

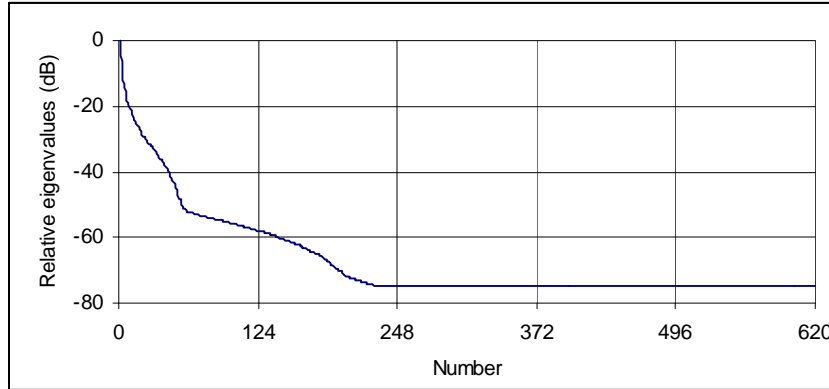
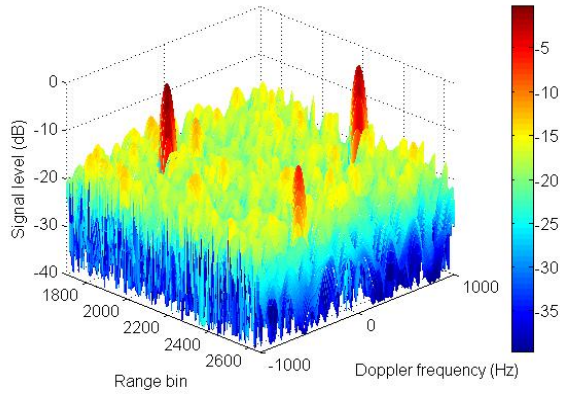


Figure 12: Eigenvalues, in descending order, of the sampled clutter covariance matrix using 800 range samples.

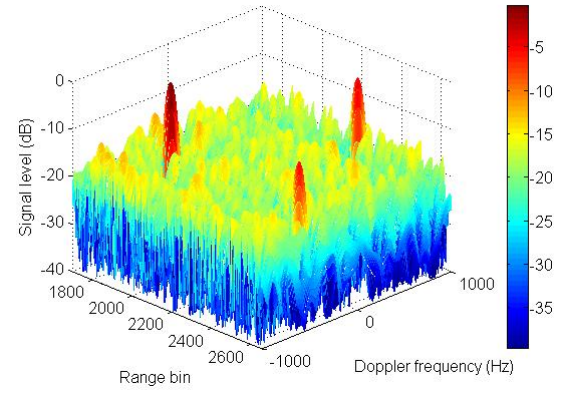
The proposed ADPCA, on the other hand, uses matrices whose dimension is $N - 1$ to estimate its parameters. As a result, it requires significantly fewer iid range samples. In addition, STAP only uses the fast-time (range) averaging processing to estimate its parameters, whereas the proposed ADPCA employs not only the fast-time but also the slow-time (pulse) averaging processing to estimate its parameters. Therefore, the proposed ADPCA is more robust in the case of reduced samples.

5.1.1 Comparison with PAMF

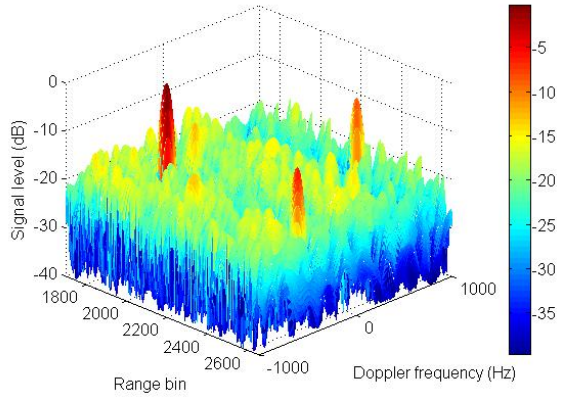
The proposed ADPCA algorithm looks similar to the PAMF algorithm (Roman, et al, 2000, Michels et al, 2003, Dong, 2006). However, there exist differences. First, the proposed ADPCA seems to be equivalent to PAMF with filtering order equal to one. PAMF with the filtering order equal to one usually does not perform very well but ADPCA does. The key point is that ADPCA utilises the principle of DPCA, whereas PAMF usually has to use a higher order of filtering to gain a good performance. Typical filtering orders are 3 to 5 (Roman, et al, 2000, Dong, 2006). An increase in the filtering order, however, also increases the size of the matrix to be inverted (the size of the matrix to be inverted is the filter order times the number of antenna elements), which in turn increases both the computational cost and the size of sample data. PAMF requires the inversion of diagonal block matrices of size N whereas the ADPCA does not have such requirement. Figure 13 and Figure 14 show the performance of PAMF with different filtering orders in which 100 (1301:3:1600) non-consecutive range samples were used. It can be seen that when the filtering order reduces to one, which is equivalent to the ADPCA algorithm, the processor fails to detect target 2. However, there is little SINR loss for target 2 if the filter order increases to 5.



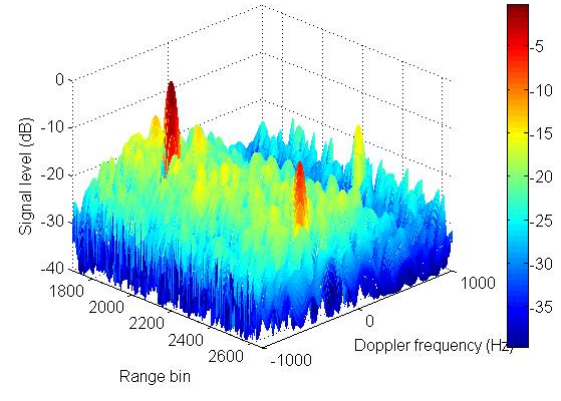
(a) filtering order = 5



(b) Filtering order = 3



(c) Filtering order = 2



(d) Filtering order = 1

Figure 13: Performance of the PAMF processor with different filtering orders.

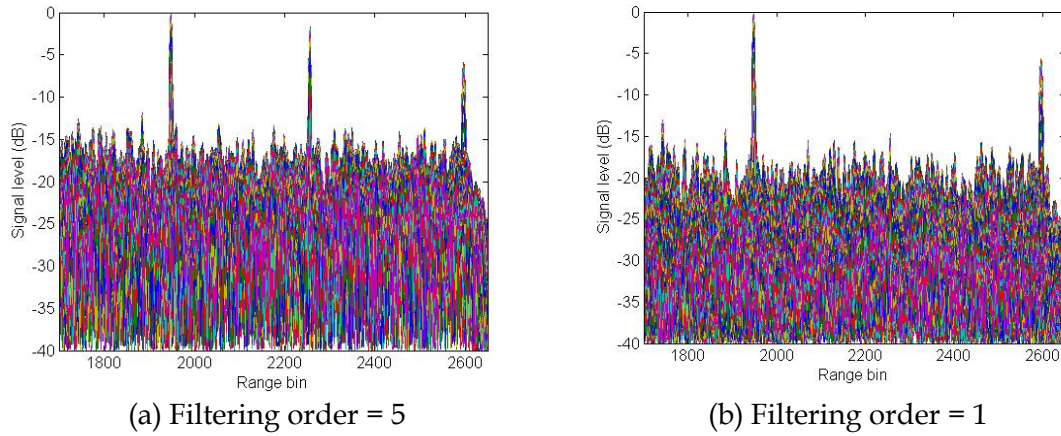


Figure 14: Performance of the PAMF processor is dependent on the filtering order. The results are plotted in the signal level versus range with the Doppler bins collapsed onto the range.

5.2 MCARM Dataset

Detailed descriptions of the MCARM system can be found elsewhere (Sloper et al, 1996, Fenner and Hoover, 1996). Some of the MCARM data analyses are also available (MITRE, 1999, RAFDCI, 1999, Sarker et al, 2001). The dataset #5-575 collected by the MCARM system was used in this report. The radar and platform parameters of #5-575 are given in Table 5 and Table 6, respectively.

Table 5: MCARM radar parameters.

| Frequency/ Polarisation | PRF | CPI | Pulse Width | Duty Cycle | Range Resolution | PRI (μ s / gates) |
|----------------------------|------|-----|----------------|---------------|---------------------|---------------------------|
| 1240 MHz/VV | 1984 | 128 | 50.4 μ s | 10% | 0.8 μ s | 504/630 |

Table 6: MCARM platform parameters.

| Height | Velocity | Illumination | Crab Angle | Antenna Tilt Angle from Horizontal ³ |
|--------|-----------|--------------|------------|--|
| 3488 m | 100.1 m/s | Side-looking | 7.28° | 5.11° |

The receiver of the MCARM system consists of 22 receiving channels (modules) organised in two azimuthally identical rows. We treated data received by one row as

³ This angle is the sum of the antenna tilt angle relative to the platform plus the recorded platform roll angle.

secondary data and the data received by the other as primary data. The physical position difference between the two rows will in general induce a phase difference between signal arrivals at the two rows. This however should impose no effect as far as generating the covariance matrix is concerned. We also only used the data collected by the first 50 pulses in the process, hence, $N = 11$ and $M = 50$ in this MCARM data study.

The antenna element horizontal spacing is 0.1092 m. With the parameters given in Table 5 and Table 6, we found $\beta = 0.924$, indicating that the data was collected under a non-DPCA condition.

Figure 15 shows the clutter profile in range after the $1/R^3$ range effect is compensated. The area illuminated by the radar mainlobe is mainly farmland with scattered houses (range bins 200-400 and 500-630, for example) and bay water (range bins 400-500, for example). The signal in range bin 68 is a replica of the transmitter signal and the useful clutter data are from around range bin 200 and beyond.

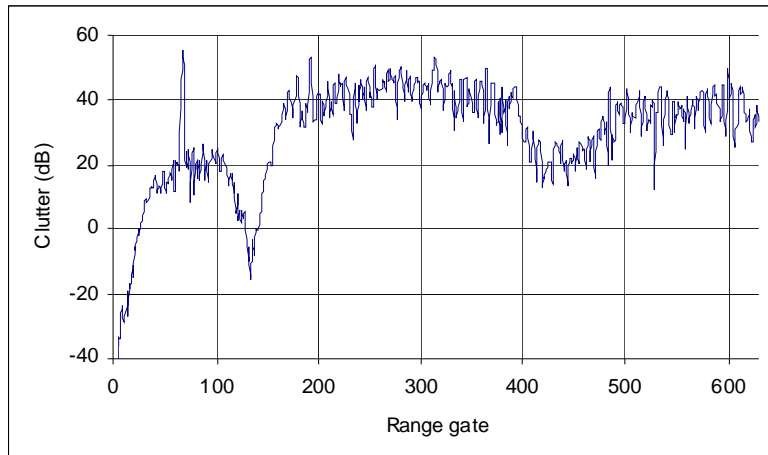


Figure 15: Clutter profile in range after the $1/R^3$ range effect was compensated.

A moving target in range bin 299 (a range ambiguous target) has been detected and reported previously (Dong, 2005). Range cells 289 to 309 were, therefore, excluded in the secondary data. An artificial moving target signal was also injected in the primary data in range bin 500 with a constant amplitude 30dB below the mean clutter of that bin and a Doppler frequency of -200 Hz.

To evaluate the performance of the proposed ADPCA processor, we first formed the covariance matrix using nearly all the possible secondary data, range bins 200 to 600 with the exclusion of bins 289 to 309. The results are shown in Figure 16. It can be seen

that all three processors have successfully detected both the genuine target in range bin 299 and the artificial target in range bin 500. However, the detection of the artificial target in the STAP processing as well as the Blum ADPCA suffers a few dB signal loss compared to the detection of the ADPCA processing. This can be more clearly viewed in Figure 17 where the figures are plotted in the signal level versus range with the Doppler bins collapsed into the range. Other evidence readily seen from Figure 16 is that there are higher signal levels in the mainlobe clutter Doppler vicinity (note that due to the aircraft's crab angle, the Doppler of the mainlobe clutter is about 150 Hz) in the results of both the STAP and Blum's ADPCA, indicating that the clutter is not sufficiently suppressed, possibly due to the insufficient range samples used for covariance matrix estimation, although all possible range samples have been used. No such evidence however is seen in the result of the proposed ADPCA.

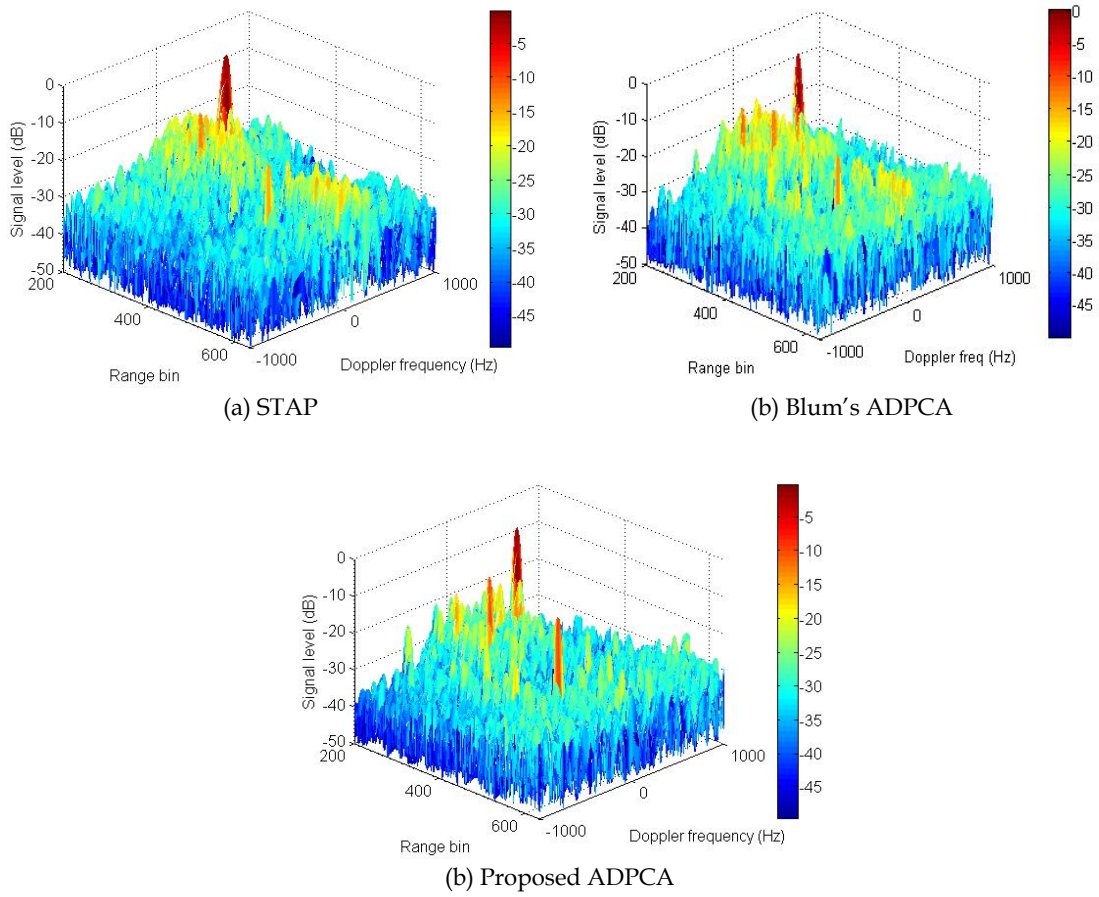


Figure 16: Detection results of MCARM data by the use of (a) STAP, (b) Blum's ADPCA and (c) proposed ADPCA. The covariance matrix was formed using approximately 400 range samples.

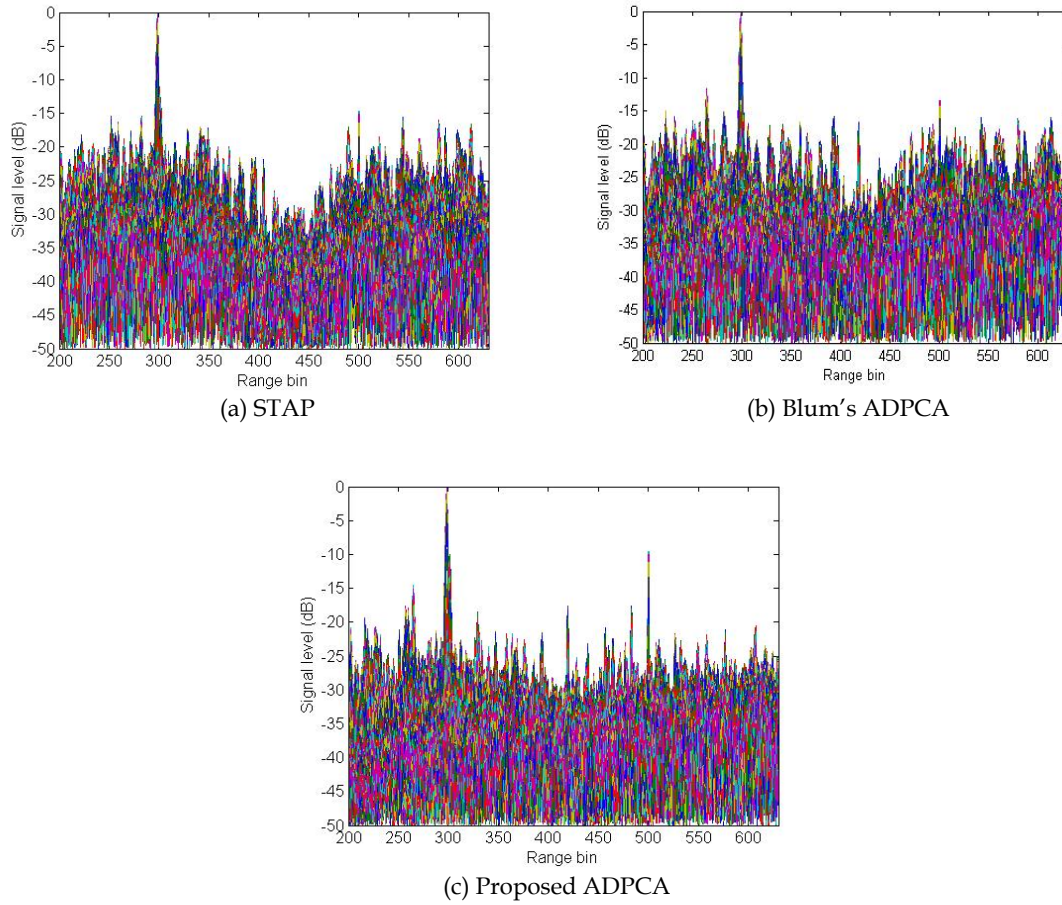


Figure 17: Detection results of MCARM data by the use of (a) STAP, (b) Blum's ADPCA and (c) proposed ADPCA. The covariance matrix was formed using approximately 400 range samples. The results are plotted in the signal level versus range with the Doppler bins collapsed into the range.

To test the advantages of the proposed ADPCA in the case of reduced samples, we greatly reduced the number of samples. The LFM bandwidth of the MCARM system was 1 MHz and the actual range sample interval was $0.8 \mu\text{s}$. To ensure that samples were statistically independent, we used every second range sample as the iid samples. Results with the use of 21 (200:2:240) non-consecutive range samples to form the covariance matrix are shown in Figure 18. Comparing Figure 18 with Figure 16, we can see that the output of STAP has been seriously distorted due to reduced range samples which cannot provide an accurate estimate of the covariance matrix and hence suppress the mainlobe clutter. The situation of the Blum ADPCA is similar, but the distortion is less severe. On the other hand, the differences between results of the proposed ADPCA shown in Figure 16 and Figure 18 are minor, indicating that the

parameters of ADPCA can be estimated at a reasonably accurate level even using reduced samples. The plots of the signal level versus range with the Doppler bins collapsed into the range are shown in Figure 19.

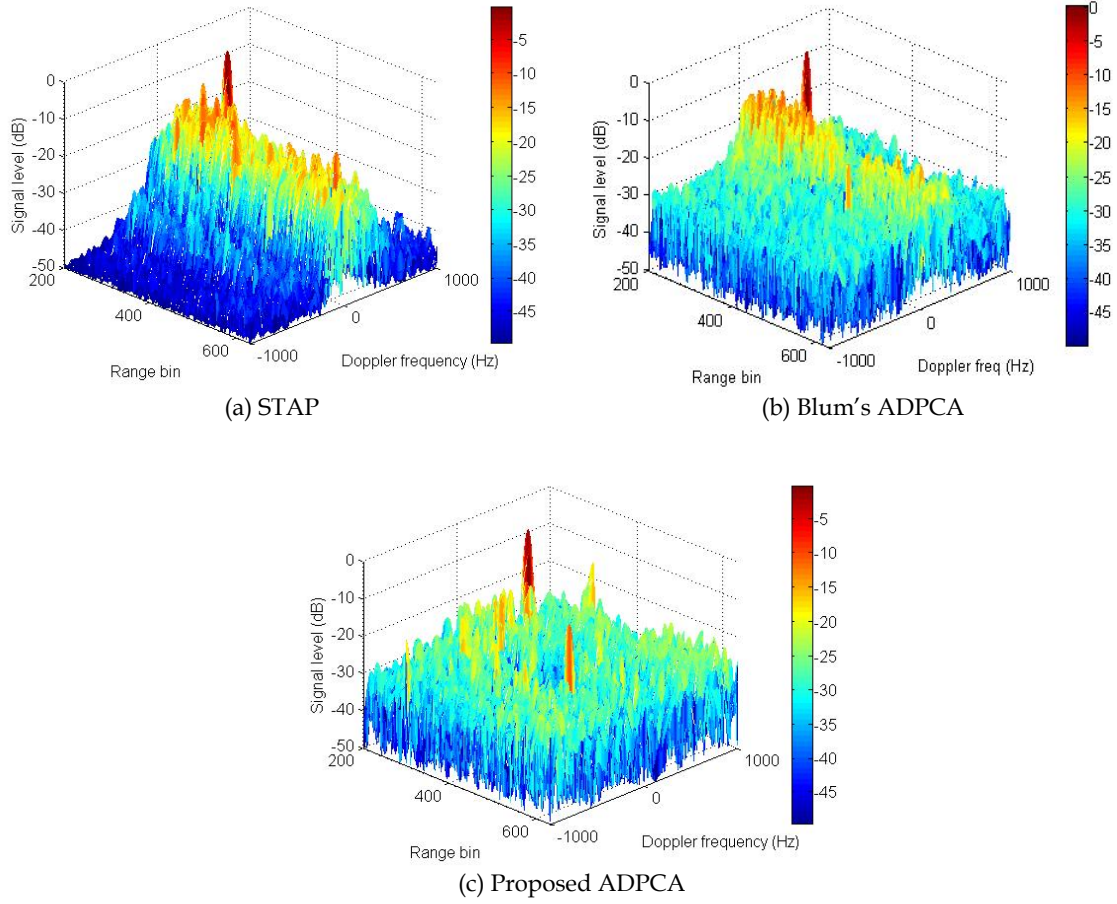


Figure 18: Detection results of MCARM data by the use of (a) STAP, (b) Blum's ADPCA and (c) proposed ADPCA. The covariance matrix was formed using 21 range samples.

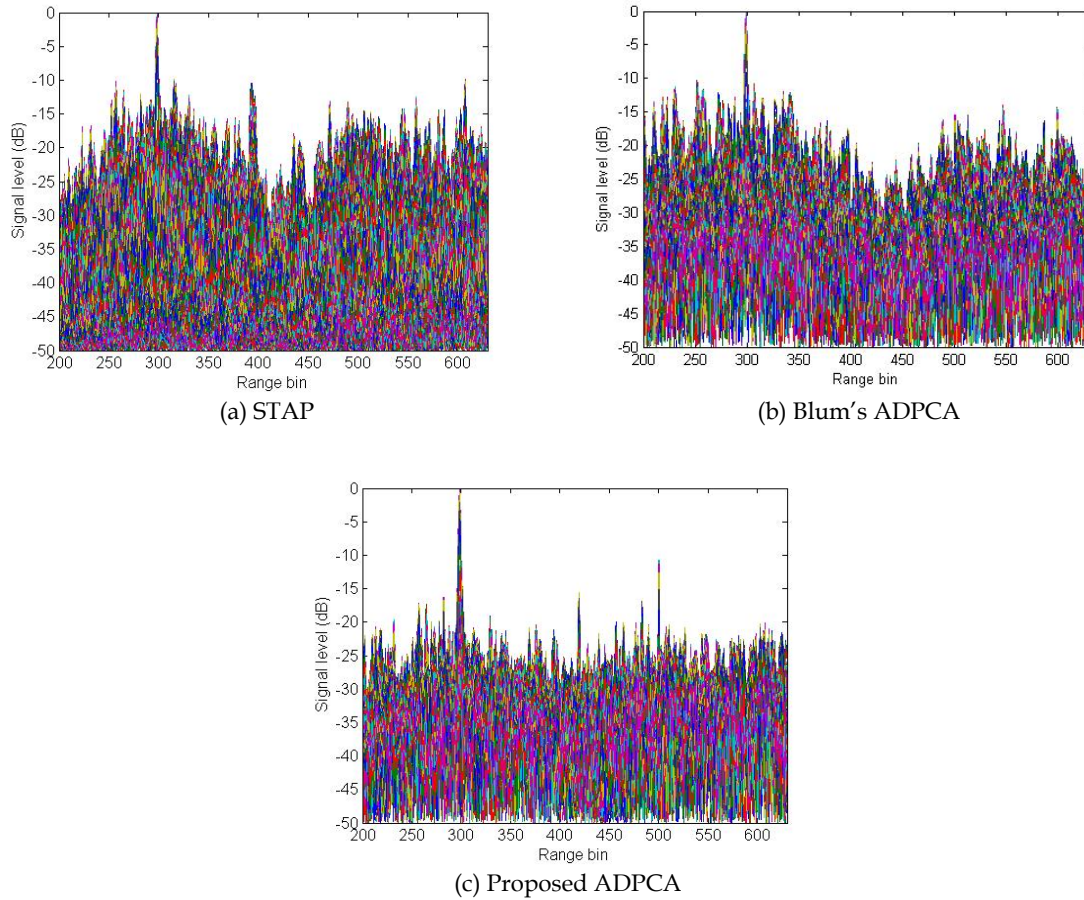


Figure 19: Detection results of MCARM data by the use of (a) STAP, (b) Blum's ADPCA and (c) proposed ADPCA. The covariance matrix was formed using 21 range samples. The results are plotted in the signal level versus range with the Doppler bins collapsed into the range.

Like STAP, the proposed ADPCA is fully adaptive to changes in the clutter environment and system parameters provided the effects of these changes have been included in the sample data used for the parameter estimation. In the above MCARM data analysis, we have seen that the proposed ADPCA is able to cope with all effects such as the antenna pattern distortion/degradation unavoidably induced by the aircraft, the shift of the Doppler frequency of the mainlobe clutter induced by the crabbing angle (as large as 7° for the MCARM dataset), the clutter notch widening induced by the clutter intrinsic motion and range foldover (see the report of Dong, 2005, for detailed discussion of the effect of the range foldover) as well as various other spatial and temporal decorrelation in the MCARM system. However we should not confuse the ability to cope with changes and the degradation of the radar performance induced by these changes. The latter is the inherent result of the effects and cannot be

recovered by any means. For instance, a crab angle of 7° of the MCARM system causes the shift of the mainlobe clutter Doppler to be about 150 Hz. As a result, any moving targets whose Doppler frequencies are in the vicinity of 150 Hz and whose echoes are not as strong as the mainlobe clutter will become undetectable. The clutter notch widening caused by the various decorrelation effects, clutter intrinsic motion and range foldover will also reduce the radar's effective detection region.

6. Conclusions

In this report we have proposed an algorithm, the adaptive displaced phase centre antenna (ADPCA), to process airborne phased array radar data for moving target detection. Its parameters are adaptively calculated by the autoregressive (AR) process. Although the name is not new, this proposed ADPCA is fundamentally different from the existing ADPCA as the former is an optimum processor whereas the latter is not. The proposed algorithm not only significantly reduces the number of samples required for estimating its parameters but also demands dramatically less computational effort with little sacrifice of the SINR loss in comparison to the conventional space-time adaptive processing (STAP). The algorithm does not have any assumptions, so it is fully-adaptive. The performance of the algorithm has been assessed using two airborne radar datasets, one generated using the high fidelity airborne radar simulation software, RLSTAP, and the other collected by the MCARM system. These two datasets were carefully chosen to cover various issues. First of all, the datasets did not satisfy the DPCA condition, so that the adaptability of the proposed ADPCA could be examined. Secondly the radar did not look in the broadside direction in the RLSTAP dataset. The second dataset was collected from a flight trial of MCARM and included effects of aircraft crabbing motion. Other decorrelation effects including radar instability, clutter intrinsic motion, range foldover and interference caused by the aircraft etc. were hence automatically included in the dataset. Therefore the evaluation of the proposed processor is realistic. The results of STAP have served as benchmarks in the evaluation.

It has been found that the proposed ADPCA performs nearly as well as STAP, suffering at most a few dB of processing gain loss in the vicinity of the Doppler of the mainlobe clutter. However if there are insufficient clutter samples to accurately estimate the covariance matrix, the performance of STAP is severely degraded whereas the proposed ADPCA still performs as well as before. Mathematically STAP requires estimation of a covariance matrix whose size is the product of the number of antenna elements and the number of pulses in a CPI. On the other hand, the proposed ADPCA estimates its parameters by the use of a covariance matrix whose size is no more than the number of antenna elements. In addition, in estimating parameters, STAP uses averaging processing only in the fast-time domain, whereas ADPCA utilises averaging processing in both the fast-time and the slow-time domains. These two differences

make the proposed ADPCA more robust and require far less sample data. In general, the parameters of the ADPCA can be satisfactorily estimated once the number of range samples is equal to or greater than twice the antenna elements. The Blum ADPCA, on the other hand, is not an optimum processor and its performance usually is poor and suffers significantly especially when the target's Doppler is close to that of the mainlobe clutter.

The operational counts (ops) required for the proposed ADPCA has been estimated. In general, it only requires 5-10% of the computation of STAP. Since most of the computation for the ADPCA algorithm is linear transforms, parallel processing and/or hardware realisation can be easily implemented. In contrast, the dominant calculation of the STAP algorithm is the inversion of the covariance matrix which is not a linear transform and limits the application of parallel processing. In this sense, computational savings of the ADPCA algorithm are even greater than the simple ops estimation and comparison presented in the report.

7. Acknowledgement

The Rome Laboratory, Air Force Material Command supplied the MCARM data and the RLSTAP software. Mr A Mahoney generated the RLSTAP data.

Detailed comments of Dr John Whitrow and some technical comments of Prof Yuri Abramovich are also acknowledged.

8. References

Blum, R S, Melvin, W L, and Wicks, M C, "An analysis of adaptive DPCA", *Proceedings of the 1996 IEEE National Radar Conference*, pp. 303-308, 13-16 May 1996.

Bresler, Y "Maximum likelihood estimation of a linearly structured covariance with application to antenna array processing", *Proceedings of the Fourth Annual ASSP Workshop on Spectrum Estimation and Modelling*, pp. 172-175, 3-5 Aug 1988.

Carlson, B D, "Covariance matrix estimation errors and diagonally loading in adaptive arrays", *IEEE Trans on Aerospace and Electronic Systems*, vol. 24, no. 4, pp 397-401, 1988.

Compton, Jr, R T, *Adaptive antennas, concepts and performance*, Prentice Hall, 1988.

Dong, Y, "Approximate invariance of the inverse of the covariance matrix and the resultant pre-built STAP processor", Research Report, DSTO-RR-291, DSTO, 2005.

Dong, Y, "Parametric adaptive matched filter and its modified version", Research Report, DSTO-RR-0313, DSTO, 2006.

Farina, A, Lombardo, P, and Pirri, M, "Nonlinear nonadaptive space-time processing for airborne early warning radar", *IEE Proc. Radar, Sonar and Navig.*, vol. 145, no. 1, pp. 9-18, 1998.

Fenner, D, and Hoover, W F, "Test results of a space-time adaptive processing system for airborne early warning radar", *Proceedings of IEEE 1996 National Radar Conference*, Ann Arbor, Michigan, 13-16 May 1996.

Gerlach, K, and Picciolo, M L, "Airborne/spacebased radar STAP using a structured covariance matrix", *IEEE Trans on Aerospace and Electronic Systems*, vol. AES-39, no. 1, pp. 269-281, 2003.

Guerci, J R, *Space-Time Adaptive Processing for Radar*, Artech House, 2003.

Isaacson, E, and Keller, H B, *Analysis of Numerical Methods*, John Wiley & Sons, Inc, 1966.

Klemm, R K, *Principles of space-time adaptive processing*, 2nd edn, IEE, 2002.

Klemm, R K (editor), *Applications of Space-Time Adaptive Processing*, IEE, 2004.

Marple, Jr, S L, *Digital Spectral Analysis with Applications*, Prentice-Hall Inc, 1987.

Michels, J R, Roman, J R, and Himed, B, "Beam control using the parametric adaptive matched filter STAP approach", *Proceedings of IEEE Radar Conference 2003*, pp. 405-412.

MITRE, "STAP processing monostatic and bistatic MCARM data", Final report prepared by MITRE, Centre for Air Force C2 Systems, Bedford, MA, 1999.

Morris, G, and Harkness, L (editors), *Airborne Pulsed Doppler radar*, 2nd edn, Artech House, 1996.

Muehe, C E, and Labitt, M, "Displaced-phase-centre antenna technique", *Lincoln Laboratory Journal*, vol. 12, no. 2, pp. 281-296, 2000.

Nohara, T J, "Comparison of DPCA and STAP for space-based radar", *Record of the IEEE 1995 International Radar Conference*, pp. 113-119, 8-11 May 1995.

RAFDCl, "MCARM/STAP data analysis", Final report, Part I and II, prepared by Research Associates for Defence Conversion Inc., New York, 1999.

Rangaswamy, M, and Michels, J H, "A parametric multichannel detection algorithm for correlated non-Gaussian random processes", *Proceedings of 1997 IEEE National Radar Conference*, pp. 349-354, Syracuse, NY, 13-15 May.

Rangaswamy, M, Michels, J H, and Weiner, D D, "Multichannel detection for correlated non-Gaussian random processes based on innovations", *IEEE Trans on Signal Processing*, vol. 43, no. 8, pp. 1915-1922, 1995.

Reed, I S, Mallett, J D, and Brennan, L E, "Rapid convergence rate in adaptive arrays", *IEEE Trans on Aerospace and Electronic Systems*, vol. AES-10, no. 6, pp. 853-863, 1974.

Richardson, P G, "Analysis of the adaptive space time processing technique for airborne radar", *IEE Proc. Radar, Sonar and Navig.*, vol. 141, no. 4, pp. 187-195, 1994.

Robey, F C, Fuhrmann, D R, Kelly, E J, and Nitzberg, R, "A CFAR adaptive matched filter detector", *IEEE Trans on Aerospace and Electronic Systems*, vol. 28, no. 1, pp. 208-216, 1992.

Roman, J R, Davis, D W, and Michels, J H, "Multichannel parametric models for airborne phased array clutter", *Proceedings of 1997 IEEE National Radar Conference*, pp. 72-77, Syracuse, NY, 13-15 May.

Roman, J R, Rangaswamy, M, Davis, D W, Zhang, Q, Himed, B, and Michels, J H, "Parametric adaptive matched filter for airborne radar applications", *IEEE Trans on Aerospace and Electronic Systems*, vol. 36, no. 2, pp. 677-692, April 2000.

Sarkar, T K, Wang, H, Park, S, Adve, R, Koh, J, Kim, K, Zhang, Y, Wicks, M C, and Brown, R D, "A deterministic least-squares approach to space-time adaptive processing", *IEEE Trans on Antennas and Propagation*, vol. 49, no. 1, January 2001.

Sloper, D, Fenner, D, Arntz, J, and Fogle, E, "Multi-channel airborne radar measurement (MCARM), MCARM flight test", Westinghouse Electronic Systems, Final Technical Report, RL-TR-96-49, vol. 1, April 1996.

Steiner, M, and Gerlach, K, "Fast converging maximum-likelihood interference cancellation", *Proceedings of IEEE 1998 National Radar Conference*, pp. 117-122, Dallas, TX, 12-13 May 1998.

Steiner, M, and Gerlach, K, "Fast converging adaptive processor on a structured covariance matrix", *IEEE Trans on Aerospace and Electronic Systems*, vol. AES-36, no. 4, pp. 1115-1126, 2000.

Van Trees, H L, *Optimum Array Processing, Part IV, of Detection, Estimation and Modulation Theory*, Wiley Interscience, 2002.

Wang, H, and Cai, L, "On adaptive spatial-temporal processing for airborne surveillance radar systems", *IEEE Trans on Aerospace and Electronic Systems*, vol. 30, no. 3, pp. 660-670, 1994.

Wang, Y L, Chen, J W, Bao, Z, and Peng, Y N, "Robust space-time adaptive processing for airborne radar in nonhomogeneous clutter environments", *IEEE Trans on Aerospace and Electronic Systems*, vol. 39, no. 1, pp. 70-81, 2003.

Ward, J, "Space-time adaptive processing for airborne radar", Technical Report, TR-1015, Lincoln Laboratory, MIT, 1994.

Ward, J, and Kogon, S M, "Space-time adaptive processing (STAP) for AMTI and GMTI radar", tutorial slides, CD of the *Proceedings of 2004 IEEE Radar Conference*, Philadelphia Pennsylvania, 26-29 April 2004.

Page classification: UNCLASSIFIED

| | | | | | |
|--|--|------------------------------|---|---|--|
| DEFENCE SCIENCE AND TECHNOLOGY ORGANISATION DOCUMENT CONTROL DATA | | | | | |
| | | | | 1. PRIVACY MARKING/CAVEAT (OF DOCUMENT) | |
| 2. TITLE Phased Array Radar Data Processing Using Adaptive Displaced Phase Centre Antenna Principle | | | 3. SECURITY CLASSIFICATION (FOR UNCLASSIFIED REPORTS THAT ARE LIMITED RELEASE USE (L) NEXT TO DOCUMENT CLASSIFICATION) Document (U) Title (U) Abstract (U) | | |
| 4. AUTHOR(S) Yunhan Dong | | | 5. CORPORATE AUTHOR Defence Science and Technology Organisation PO Box 1500 Edinburgh SA 5111 | | |
| 6a. DSTO NUMBER DSTO-RR-0334 | | 6b. AR NUMBER AR-014-074 | | 7. DOCUMENT DATE December 2007 | |
| 8. FILE NUMBER 2008/1002749 | | 9. TASK NUMBER AIR 05/264 | | 10. TASK SPONSOR OC AEWCSPD DMO | |
| | | | | 11. NO. OF PAGES 54 | |
| | | | | 12. NO. OF REFERENCES 36 | |
| 13. URL on the World Wide Web http://www.dsto.defence.gov.au/corporate/reports/DSTO-RR-0334.pdf | | | | 14. RELEASE AUTHORITY Chief, Electronic Warfare and Radar Division | |
| 15. SECONDARY RELEASE STATEMENT OF THIS DOCUMENT Approved for Public Release OVERSEAS ENQUIRIES OUTSIDE STATED LIMITATIONS SHOULD BE REFERRED TO DOCUMENT EXCHANGE, PO BOX 1500, EDINBURGH, SA 5111, AUSTRALIA | | | | | |
| 16. DELIBERATE ANNOUNCEMENT No Limitations | | | | | |
| 17. CASUAL ANNOUNCEMENT Yes | | | | | |
| 18. DSTO RESEARCH LIBRARY THESAURUS Airborne radar Space-time adaptive processing Phased array radar | | | | | |
| 19. ABSTRACT Employing the autoregressive (AR) technique and the principle of displaced phase centre antenna (DPCA) we construct an optimum adaptive DPCA processor for moving target detection from airborne phased array radar data collected under non-DPCA conditions. It is fundamentally different from the existing adaptive DPCA which is not optimum. The number of range samples it needs to estimate its parameters is only approximately twice the number of antenna elements, significantly smaller than the number required by the conventional space-time adaptive processing (STAP) and other algorithms. Computationally it only requires 5-10% cost of STAP. The processor is tested using both the simulated and genuine airborne phased array radar data. With ample samples, its performance approaches optimum. In the case of reduced samples, it considerably outperforms STAP and others examined. | | | | | |

Page classification: UNCLASSIFIED